DESIGN AND FABRICATION OF A HYBRID DARRIEUS-SAVONIUS MIRCO HYDROKINETIC TURBINE

A Final Year Project Report

Presented to

SCHOOL OF MECHANICAL & MANUFACTURING ENGINEERING

Department of Mechanical Engineering

NUST

ISLAMABAD, PAKISTAN

In Partial Fulfillment
of the Requirements for the Degree of
Bachelors of Mechanical Engineering

by

Umar Farooq
M Nauman Saeed
Farhan Rafique

June 2018

EXAMINATION COMMITTEE

We hereby recommend that the final year project report prepared under our supervision by:

UMAR FAROOQ	NUST-2014-32345BSMME11114F.
M NAUMAN SAEED	NUST-2014-32932BSMME11114F.
FARHAN RAFIQUE	NUST-2014-32912BSMME11114F.

Titled: **"DESIGN AND FABRICATION OF A HYBRID DARRIEUS-SAVONIUS MIRCO HYDROKINETIC TURBINE"** be accepted in partial fulfillment of the requirements for the award of BACHELORS OF MECHANICAL ENGINEERING degree.

Supervisor: Dr. Muhammad Sajid, Assistant Professor, Department of Mechanical Engineering, SMME.	Dated:
Committee Member: Dr Emad Uddin, Assistant Professor, Department of Mechanical Engineering, SMME.	Dated:
Committee Member: Dr Zaib Ali, Assistant Professor, Department of Mechanical Engineering, SMME.	Dated:

_____ _____

(Head of Department) (Date)

COUNTERSIGNED

Dated: _____ _____

(Dean / Principal)

ABSTRACT

The project was initiated with an objective to design a power generation system that could easily be used in an open channel flow. The main targeted areas of the operation of this system were rivers and canals. We had an aim to design and fabricate a hydrokinetic turbine which would be able to generate an output of 5kW. Initially, the strategy was to design and fabricate a micro hydrokinetic turbine as a prototype, with small power output capacity and then to scale up this model after certain tests, relatively larger hydrokinetic turbine which would be able to provide the desired power output.

In the designing phase of the micro hydrokinetic turbine, a number of turbines were studied and based upon the characteristics of different turbine types, it was decided that the vertical hydrokinetic turbines had the potential to serve our purpose in a more effective manner. Furthermore, it was decided to go with an idea of designing a self-starting and high torque transmitting, hybrid hydrokinetic turbine.

The prototype was designed according to the available water velocity in the SMME water tunnel i.e. $0.5ms^{-1}$. After the completion of fabrication process a number of tests were conducted and conclusions were drawn, based upon which the prototype model was to be scaled up to a larger hydrokinetic turbine to be operated in rivers and canals with the ability to provide the desired power output of 5kW.

PREFACE

A hydro turbine is a type of turbine that is used to extract energy from water and convert it into the rotational energy of the shaft. Our focus is the hydrokinetic turbine which typically extracts the energy of the flowing water (low head) by reducing its velocity and converts it into the rotational energy of its rotating shaft. With respect to any particular hydro site the process of selecting a hydrokinetic turbine is mainly dependent on the flowrate of the flowing water and whether the specified turbine will be capable enough to meet the target power output in off design conditions or not. A power-speed characteristic exists for every turbine i.e. a certain turbine will have its maximum coefficient of performance at a particular combination of its tip speed ratio, flow velocity and some other important parameters.

Turbines can be classified on in many different types depending on the basis of their operation. This report represents our process of designing and fabricating a hydrokinetic turbine which can be used in open channel canals, rivers and other flowing water bodies in order to provide electricity to the power sector and areas nearby these flowing water bodies.

ACKNOWLEDGMENTS

Above all, we would thank Allah Almighty, for He bestowed upon us the necessary knowledge and dedication to complete this project. We would also like to thank our faculty advisor, AP Dr. Muhammad Sajid for his endless assistance at each and every step. We would also like to thank our co-supervisors especially AP Dr. Emad Uddin for his shear guidance in the designing phase of our hydrokinetic turbine. Apace with others, we would also like to thank Mr. Mujahid (MS student) for all his help during the testing phase elated to the availability of the water tunnel.

We would really like to thank our parents for all their prayers because of which we were able to complete this project with flying colours of success.

ORIGINALITY REPORT

We hereby certify that this research work titled **"Design and Fabrication of a Hybrid Darrieus-Savonius Micro Hydrokinetic Turbine"** is our own work. This work has not been presented elsewhere for assessment. All material which has been used from other sources has been properly acknowledged/cited.

Umar Farooq

NUST201432345BSMME11114F

M Nauman Saeed

NUST201432932BSMME11114F

Farhan Rafique

NUST201432912BSMME11114F

COPYRIGHT

TABLE OF CONTENTS

LIST OF TABLES

LIST OF FIGURES

ABBREVIATIONS

RCT	River current turbines
RCECS	River current energy conversion systems
tsr	Tip speed ratio
rpm	Rotation per minute
AOA	Angle of attack
A.R	Aspect ratio
DMSV	Double multiple streamtube with variable interference factor

NOMENCLATURE

F_L	Lift force
F_D	Drag force
F_T	Tangential force
F_N	Normal force
C_N	Coefficient of normal force
C_L	Coefficient of lift force
C_D	Coefficient of drag force
C_T	Coefficient of tangential force
A_s	Swept area
ρ	Density
v	Velocity
α	Angle of attack
C_P	Coefficient of performance or Power coefficient
P_T	Power extracted by turbine rotors
P_A	Total power available in flowing water
v_{in}	Incoming flow velocity
ω	Angular speed of turbine rotor
R	Rotor radius
h	Blade length
σ	Solidity
N_b	Number of blades
c	Chord length
d	Rotor diameter
λ	Tip speed ratio
v_{in}	Incoming velocity of flowing water
V_o	Free stream velocity
a_u	Upstream interference factor
V_u	Upstream induced velocity
V_e	Equilibrium induced velocity
V_d	Downstream induced velocity
a_d	Downstream interference factor
W_u	Resultant flow velocity
TSR	Local tip speed ratio
θ	Azimuthal Angle
Re_b	Local Reynolds number
K_v	Kinematic velocity
α_o	Initial angle of attack
fup	Constant for characterizing the upstream flow conditions
N	Number of blades

T_{av}	Average torque
Ct_{av}	Coefficient of average torque
Cpu	Upstream power coefficient
Cpd	Downstream power coefficient

CHAPTER 1: INTRODUCTION

1.1 Turbine:

A turbine is a mechanical device which converts the kinetic energy of a flowing fluid into the rotational energy of its rotor. The flowing fluid may be water, steam, gas, air or any other fluid. The rotor of the turbine may be a shaft of a drum with blades attached to it. The flowing fluid strikes with the blades of the turbine and imparts a fraction of its energy to the blades which in turn rotate the shaft/drum of the turbine. On the basis of flowing fluid type commonly the turbines are either wind turbine or water turbines (also known as hydro turbines).

1.2 Working Principle:

The working principle for the turbines is very simple that is when the incoming fluid strikes the blades of the turbine, it causes the blades to be displaced producing rotational motion. The shaft of the turbine is directly coupled with to an electric generator thus the energy of the flowing water is converted into electric energy. The electric power extracted from water is known as hydroelectric power.

1.3 Background:

Micro hydrokinetic turbine is a turbine which produces electric power ranging from 5kW to 100kW using the kinetic energy of the flowing water. The turbines with a nominal power output of less than 5kW are known as Pico hydrokinetic turbines. Hydrokinetic turbines can be used to electrify nearby houses, resorts, hotels, etc. located near to flowing water bodies such as rivers and canals. On a larger scale they may also be used to provide electricity to the power sector. The process of electricity generation through hydrokinetic turbines has a larger scope mainly in all the developing countries of the world as they are able to provide an economical and green source of energy.

These low head hydro turbines use kinetic energy of water thus eliminating the need of generating an artificial head. This type of energy production is environment friendly and poses no damage to marine life.

1.4 Aims and Objectives:

The micro hydrokinetic turbines have the capability to be installed easily in all flowing water bodies without the need of any water proof generator or complex manufacturing processes.

The main objective was to **design and fabricate a hybrid Darrieus-Savonius micro hydro turbine.** The turbine was designed in a way that it operates on the designed tip speed ratio which is set according to the flow conditions in order to get the maximum output from it.

The effect of the following parameters on the overall coefficient of performance of the micro hydrokinetic turbine are studied in this report.

- Solidity
- Frontal area
- NACA profile
- Number of blades
- Aspect Ratio

1.5 Research Methodology:

Before moving to the designing process, it is compulsory to understand the basic concepts and parameters which are necessary in order to determine the output of the turbine. This was done by studying the literature review of the turbines in detail. After selecting the type of the turbine, a number of different parameters effecting the efficiency of the turbine were studied and the set of specific parameters which resulted in the maximum value of coefficient of performance was chosen.

CHAPTER 2: LITERATURE REVIEW

2.1 Need for the micro hydrokinetic turbine:

The canal system of Pakistan is regarded as one of the best among others worldwide consisting of 12 linked and 45 normal canals therefore it is a great source for renewable energy in our country. Pakistan has an abundant supply of free streams and rivers especially on the northern side of the country. As far as the scattered and isolated villages of northern areas are concerned, there is no proper electric supply available in these areas. Furthermore, the poor residents rely on pinewood sticks and costly kerosene lamps thus making a precarious substitute for the lack of electricity.

Low head hydropower applications use rivers or canals to produce energy. These applications may not need to dam or retain water to create hydraulic head. Using the drop in a river flow to create electricity may provide a renewable energy source that will have a minimal impact on the environment.

2.2 Hydrokinetic turbine and types:

Hydro turbine converts the water energy into mechanical energy and the mechanical energy is later on converted to electrical energy by means of a generator. Now, as described earlier, hydro kinetic turbines utilize a fraction of the total kinetic energy of the flowing water and convert it into mechanical energy in form of rotational energy of the turbine shaft. There is no special civil structure required in order to extract hydro energy through this means. Unlike Francis and Pelton turbines, hydrokinetic turbines are very different from the conventional turbines. In past few years, several new concepts of hydrokinetic turbines have been developed so far in order to extract energy from free flowing water bodies. Such hydrokinetic turbines have taken over the world in terms of their economic feasibility and easy to commercialize capability. Hydrokinetic turbines which are deployed in rivers are commonly known as river current turbines (RCT) or river current energy conversion systems (RCECS).

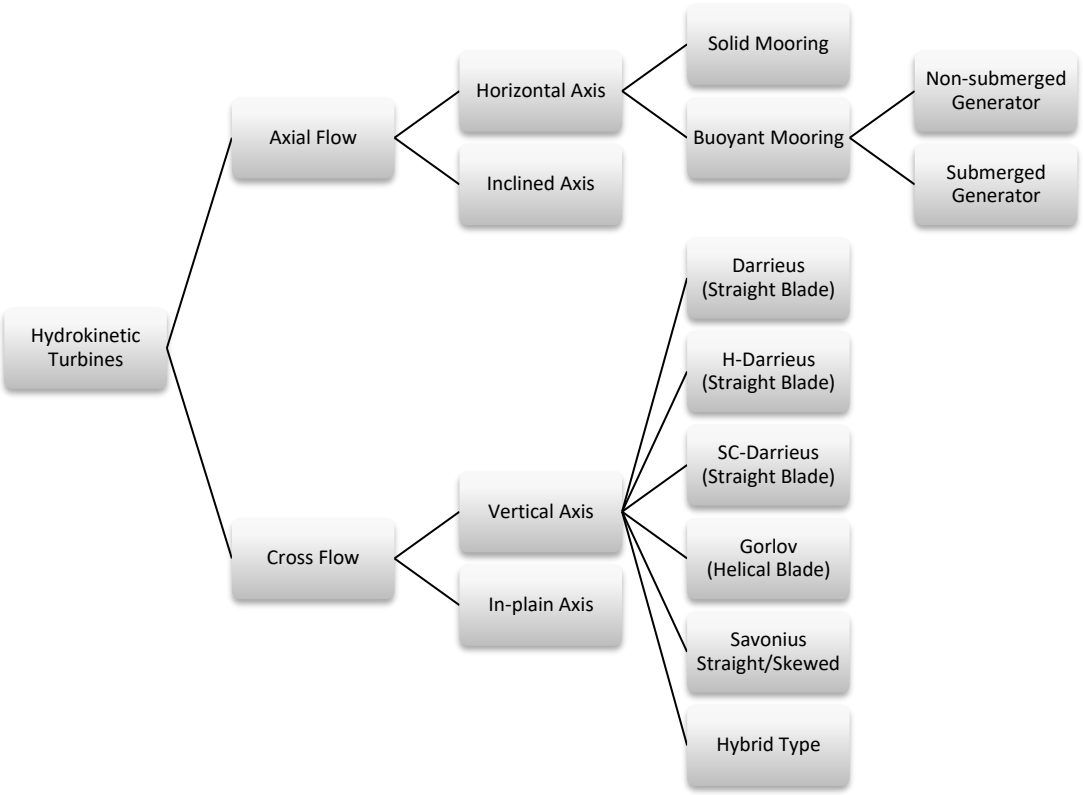

Figure 1: Classification of Hydrokinetic Turbines

Depending upon the direction of axis of rotation of hydrokinetic turbines with respect to the direction of the flowing water, these turbines are broadly classified into two main categories; they are axial flow turbines and crossflow turbines.

Axial Flow Turbines:

In axial flow turbines the direction of the rotational axis of the rotor is parallel to that of the flowing water. Axial flow hydrokinetic turbines may consist of two, three or multi-blades.

Crossflow Turbines:

In vertical axis or cross flow turbines, the direction of the rotor axis is orthogonal to that of the water flow. Vertical Turbines can be broadly divide into two categories.

1. Lift Type Turbines
2. Drag Type Turbines

Lift Type Turbines:

In this type of turbines, the energy is extracted from the flowing water by a component of the lift force working in the rotational direction of the rotor. The lift force thus produced is perpendicular to the resultant component of the relative velocity and the water velocity. It has been studied that in crossflow type hydro turbines, Darrieus turbines have the highest values for efficiency. Also a very high tip speed ratio (tsr) can be achieved in Darrieus turbines which results in high rpm.

Figure 2: H-Darrieus Turbine

Drag Type Turbines:

In this type of turbines, the energy is extracted from the flowing water by a component of the drag force. A typical example of such devices is a Savonius turbine in which drag force is generated usually when the flowing water strikes the concave and convex part of

the semi-spherical blades. Drag based turbines are generally considered less efficient as compared to the lift type turbines as their flow energy utilization is lower than that of the lift type ones. This is the reason why the drag type devices are generally used for low power applications. Savonius hydrokinetic turbines can be deployed in regions even with very low flowrates with ranging flow velocities from $0.5ms^{-1}$ [1-3].

Figure 3: Savonius Turbine

A study was conducted by Guney and Kaygusuz in order to study the hydrokinetic turbine types in detail and it was concluded that axial axis water turbines may have the self-starting ability and a higher efficiency but they are quite costly and complex in terms of fabrication and transportation and they also require water sealed generators. On the other hand, vertical axis hydrokinetic turbines are simple to manufacture, lighter to transport (simple, light and portable structure) and do not require water sealed generators thus making them economically more feasible [4].

2.3 Comparison between axial and vertical turbines:

The comparison between axial and vertical axis hydrokinetic turbines indicate that for the case of free flow applications, vertical axis hydro turbines are more feasible than the axial ones therefore, in order to extract energy from rivers, industrial flow and irrigation canals vertical axis turbines are mostly used. Due to the widespread advantages of small sized blades and low costs of manufacturing, transportation and maintenance vertical axis hydro turbines are preferred to be used in free flow water streams to supply electricity to the nearby areas [5]. Commonly, Darrieus and Savonius type turbines are used in river energy applications [5]. Vertical axis hydrokinetic turbines are known for river based applications whereas horizontal ones are known for extraction of tidal energy from oceans. Furthermore, in vertical axis, Darrieus turbines are usually preferred. In Darrieus type, H-Darrieus and Squirrel-cage Darrieus turbines are mostly used. In many aspects vertical axis turbines have many advantages over the horizontal ones [6].

Table 1: Comparison between the Axial Flow and Cross Flow

Characteristics	Axial Flow	Cross Flow
Efficiency	High	Low
Self-starting Capability	Present	Absent
Cost (Manufacturing, Transportation, Maintenance)	High	Low
Shape of Rotor	Disc Type	Cylindrical type
Hydrofoil Shape	Necessary	Not necessary
Blade Size	Large	Small and simple
Debris Problems	Clogged with debris	Able to deflect debris
Other Requirements	Water sealed components required	No such requirements
Installation Ability	Single unit only due to disc-shaped rotor. Impossible to deploy in small, narrow rivers.	Can be stacked together to deploy in bigger rivers.

2.4 Selecting The Vertical Type Hydrokinetic Turbines:

The idea for going with the axial type of hydrokinetic turbines was ruled out because of the following reasons:

- High Cost
- Complexity in Fabrication
- Suitable for High Flow Rates
- Limitation of Resources
- Water-Sealed Generator

It was decided to go with the vertical type of hydrokinetic turbines because of the following reasons:

- Low Cost
- Simplicity in Fabrication
- Suitable for Low Flow Rates
- Limitation of Resources
- Easy Generator Coupling

2.5 Technique of Hydropower Extraction:

In order to extract energy from the hydro currents the following two methods are mainly utilized:

Traditional Hydro Technology:

It utilizes the potential energy of water from head differences in order to extract power. This is usually accomplished by constructing dams and other water storages. It must be noted here that the dams and all other barriers of water storages impact negatively on the environment and they produce considerable amount of ecological problems including the blockage of fish migration paths and modification in the climate in their vicinity [7, 8]. Also, the process of construction of dams is too much costly, it effects wildlife and requires large areas [9].

The Hydrokinetic Technology:

This method utilizes the kinetic energy of water in order to extract power from it. The devices used based on this concept are termed as Hydrokinetic Devices. It is relatively a new technique to extract hydro power with minimal environmental effects [10]. Owing to the simplicity and environmental friendliness of these devices, they are widely used in order to generate electricity for remote power applications [11].

2.6 Hydrokinetic Turbines:

Water moving in canals and river streams possess kinetic energy. In order to extract this kinetic energy, several technologies have been adopted including buoy or float systems. One of the most widely used technology is the use of hydrokinetic turbines. These devices are used in order to extract a part of the kinetic energy of the flowing water to generate electricity. The concept of hydrokinetic turbines is being widely utilized for in-land as well as marine water bodies. The traditional way of extracting energy from water requires the generation of artificial water head using costly methods such as building dams whereas this new advancement in the field of renewable energy makes energy extraction from water possible without disturbing the natural pathway of the water streams [12].

2.7 Advantages and Limitations:

Advantages of Hydrokinetic Turbines:

- **Efficiency:**
  Even with a very limited flowrate (as small as two gallons per second) electric current can be generated using a micro hydro kinetic turbine. This electricity can be transferred to far off places where it can be used.
- **Continuous Source of Electricity:**
  Relative to other small scale renewable energy systems, hydrokinetic turbines are a far more reliable source of electricity.
- **No Special Arrangements Required:**
  Hydrokinetic turbines use the water from a running river or a canal and that water is redirected into the water body after passing through the turbine rotors thus hydrokinetic turbines have negligible effects on the surrounding ecosystem.
- **Inexpensive Source of Energy:**
  A much small amount of investment is required in order to build a small scale hydrokinetic turbine as compared to other hydro turbines. The maintenance fees of this type of turbine are also very small in comparison to other hydro power sources.
- **Scope in Underdeveloped Countries:**
  Owing to the low installation and maintenance costs of micro hydrokinetic turbines, there is a large scope of this technology in the developing countries of the world where energy crises are high and energy sources are expensive such as in small towns and other rural areas.
- **Power Supply:**
  At any area, if the flow of water is relatively good and this technology is implemented on a large scale, it can produce a large amount of power which can be supplied to the power supplying companies.

Limitations:

- **Site Conditions:**
  There are a lot of factors contributing to the efficiency of this technology which depend upon the site conditions in which the turbine is installed. These factors include distance from the power source, flowrate of the stream, size of the flowing stream.
- **Increase In Energy Demand:**
  The physical size and the water velocities in the streams limit the power output of the micro hydrokinetic turbines.
- **Inconsistency in Flowrate:**
  Throughout the year, the water flowrate will never remain consistent and will result in the reduction of the total power output of the micro hydrokinetic turbines. A relatively higher level of research work is required in order to resolve this issue to make sure that the energy demand is met throughout the year.
- **Effects on Ecosystem::**
  Micro hydrokinetic turbines do not affect the environment on a considerable level however, proper care must be taken while planning for the construction of the infrastructure of these micro hydrokinetic turbines.

Why Hydrokinetic Turbines:

The canal system of Pakistan is regarded as one of the best among others worldwide therefore it is a great source for renewable energy in our country. Low head hydropower applications use rivers or canals to produce energy. These applications may not need to dam or retain water to create hydraulic head. Using the drop in a river flow to create electricity may provide a renewable energy source that will have a minimal impact on the environment.

Comparison with Wind Turbines:

As far as the operation, electrical hardware and speed capability for maximum performance is concerned, hydrokinetic and wind turbines are treated very closely [13]. The density of water is much higher than that of air, almost by a factor of 800% which equalizes the performance of a wind turbine operating at a wind velocity of 110mph to that of a hydrokinetic turbine operating at a water velocity of just 12mph [14] making hydrokinetic turbines much more efficient than wind turbines even at low flow velocities. Also, one of the drawbacks of wind turbines is that they require a large area of land in order to operate whereas hydrokinetic turbines have the ability to operate under water making them independent in this aspect [15].

2.8 Advantages of Vertical Axis Wind Turbines:

One of the main advantages of vertical axis turbines is that they can receive flow from any direction because their axis of rotation is always orthogonal to the direction of water flow whereas horizontal axis have their axis of rotation inline to the flow direction so they are dependent on the flow direction, as a result in vertical axis turbines yaw mechanism is not needed, vertical axis turbines are much more quieter in operation and are relatively simpler than horizontal axis turbines in terms of mechanical complexities and more cost effective generator coupling costs because the generator in vertical axis turbines is placed outside water[16-18].

Increasing the overall size of the turbine is a key factor in increasing the overall power output of a turbine which in case of vertical axis turbines is easier to do whereas in case of horizontal axis turbines increasing the size of the blades gives rise to an increase in the gravitational stresses at the roots of the blades.

2.9 Savonius Hydrokinetic Turbine:

Working Principle:

In the Savonius type vertical axis hydro turbine the drag coefficient for the concave side is more relative to its convex side therefore the advancing concave side blade will experience more drag than its returning convex side [19]. In the Savonius turbine, the advancing flow blade side develops a drag force and its opposite side i.e. the returning one develops a returning force from the opposite direction through the overlap (gap) generating a pair of forces coupled together which generates torque and power [5].

2.10 Savonius Wind Turbines and Savonius Hydrokinetic Turbines:

Savonius wind turbine and Savonius hydrokinetic turbine are geometrically analogous in terms of physical operations of energy extraction although the density of water is 835 times than that of air which enables the Savonius hydrokinetic turbines to extract enough energy even at very low flowrates [20], thus their design or geometric parameters that effect their performance are also the same. Several design parameters have been optimized numerically or experimentally by researchers in order to enhance the performance of the rotor including end plate, aspect ratio, overlap ratio, Reynolds number, multi-staging, blade shape, number of blades, rotor angle, tip speed ratio, etc. On the other side geometric and installation parameters including the direction of rotation and the clearance ratio either clockwise or counterclockwise can also affect the overall performance of the turbines [5].

2.11 Factors effecting the performance of Savonius/Darrieus Turbines:

Following are the factors effecting the performance of Savonius/Darrieus Turbines:

Swept Area:

The section of the flowing fluid which faces/encloses the turbine forms the swept area of that turbine. For all vertical turbines it has a rectangular shape and is calculated as:

$$A_s = h \times d \tag{1}$$

The swept area actually sets an upper limit to the volume of fluid passing through the turbine. It is directly proportional to the to the output power of the turbine.

Diameter:

It is observed that at low rotational speeds the turbines with bigger diameter generate more torque and the turbines with smaller diameter generate less torque [21].

Number of Blades:

The overall smoothness of the operation of rotor mainly depends on the number of blades. A number of studies conducted suggest that for a vertical axis the number of blades must be equal to two or three for the maximum performance.

Solidity:

The ratio of total blade area to the projected turbine area is known as solidity 'σ' of a turbine. Mathematically it is represented as:

$$\sigma = \frac{N_b \times c}{d} \tag{2}$$

Solidity directly effects the self-starting abilities of a turbine, it has been found that turbines with the solidity ratio of 0.4 and above have the ability to self-start [22].

Initial Angle of Attack:

The angle of the blade with regard to its trajectory forms the initial angle of attack of the turbine blade. If the leading edge of the blade is towards the inside of the circumference of its trajectory, the angle is considered as to be negative and vice versa.

Aspect Ratio:

The aspect ratio for any turbine is defined as the ratio of the length of blade to the turbine rotor's radius.

$$A.R = \frac{h}{R} \tag{3}$$

A Darrieus turbine with a low value of aspect ratio has certain advantages like higher coefficient of performance, thicker blade (a structural advantage having less height and more chord) and greater stability from greater moment of inertia [23].

It is observed that Savonius turbines having a higher aspect ratio are more efficient because of low losses than those with a low aspect ratio. Owing to various structural reasons Savonius turbines are usually installed with low aspect ratios but their performance is improved using end plates [5]. Aspect ratio of a Savonius turbine effects the turbine in such a way that with increase in aspect ratio, increases the angular acceleration of the turbine while decreasing the rotor momentum and inertia [24]. A number of studies have been conducted for wind and water as the working fluid which show that the optimum value for the aspect ratio of Savonius turbines ranges from 1.0 to 2.0 [25-35]. Increasing the aspect ratio of the turbines increases the performance of the turbines, in case of Savonius rotor the performance keeps on increasing with the aspect ratio till AR=6.0 after which it starts decreasing. Hence, it is concluded that the best possible performance of the Savonius rotor is achieved at the aspect ratio of 6.0 [5].

End Plates (Savonius):

The overall performance of a Savonius hydro turbine is found to increase significantly by using end plates [17, 36-38]. The function of the end plates is to prevent the leakage of

the fluid from the concave side blade in order to keep the pressure difference between both the sides at satisfactory levels throughout the height of the rotor [17]. An experimental investigation was conducted by Sivasegaram in order to study the optimum size for the end plate diameter and it was found that the optimum value for it is 1.1 times the diameter of the rotor [39]. Circular end plate maximizes the coefficients of power and torque for the Savonius turbines (Helical). The overall power coefficient of a Savonius turbine increases by 36% as a result of using both the upper as well as the lower end plates relative to a turbine with no end plates [5]. In Savonius rotor the function of end plates is to prevent the fluid leakage from the concave side of the blades to the external flow in order to keep the pressure difference between the convex and concave sides of the blade at satisfactory levels throughout the height of the rotor [17]. The optimum value for the end plate diameter is 1.1 times of diameter of rotor.

Gap Ratio and Overlap Ratio (Savonius):

In Savonius turbines gap ratio is defined by the relative distance between the centers of the circular blades. If the blades of the Savonius turbine are merged into one another, it is said to be a positive overlap whereas if the blades are far apart, the Savonius is said to be negatively overlapped.

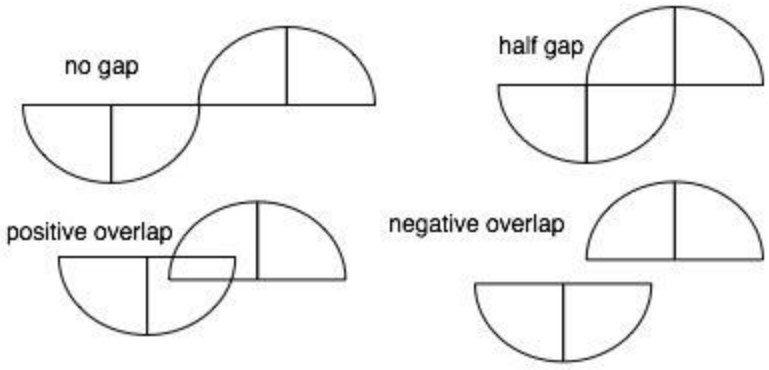

Figure 4: Savonius Turbine (Gap Ratio and Overlap Ratio)

2.12 Selection Criteria:

In the vertical type of hydrokinetic turbines, the selection criteria were based on the following attributes/characteristics:

- Coefficient of Performance
- Manufacturability
- Starting Torque

Based upon these points, it was concluded that the hybrid Darrieus-Savonius Hydrokinetic Turbine serves the purpose in the best possible way as the combination has the ability to generate self-starting torque, it is easy to manufacture and has a high coefficient of performance.

2.13 Why Hybrid Darrieus-Savonius Turbine:

Darrieus Turbines (lift type) are known for their high rotational speeds but they lack the ability to self-start that is an external power source is always required by them to initialize their motion.

Savonius Turbines (drag type) are well known for their self-starting ability but they are not capable enough to generate high rpm thus are limited to high torque low rotational speed applications.

Therefore, a hybrid Darrieus-Savonius Hydrokinetic Turbine is selected because it is more power efficient and has better self-starting ability as well as a high torque coefficient than any of the single rotor [23].

The efficiency of the Hybrid Darrieus-Savonius Hydrokinetic turbine is to be further improved by free wheel mechanism.

Figure 5: Hybrid Darrieus Savonius Hydrokinetic Turbine

Free Wheel Mechanism:

A free wheel mechanism is a device which has the ability to disengage the driving shaft and the driven shaft when the driven shaft rotates at a relatively higher speed than the driving shaft. In our case, Savonius turbine is considered as the driving shaft and Darrieus turbine is considered as the driven one. When the system is in its initial phase, the Savonius turbine generates the starting torque. At this instant, both the Savonius and Darrieus turbine shafts are engaged resulting in the rotation of the Darrieus turbine along with the Savonius turbine. A point comes when the initial startup torque required by the Darrieus turbine is received and at this point the Darrius turbine starts rotating at a higher rotational speed and at this instant the shafts of both turbines are disengaged from one another thus enabling the Darrieus turbine to rotate freely with higher rotational speeds. In this way, the required starting torque condition for the Darrieus turbine is fulfilled by coupling it with a Savonius turbine in a hybrid Darrieus-Savonius Hydrokinetic Turbine System.

CHAPTER 3: METHODOLOGY

3.1 General Lift and Drag Forces:

Lift is the force that is orthogonal to the resultant velocity vector whereas this resultant velocity vector is a result of the relative velocity vector and the actual incoming flow velocity vector. Lift force is generated due to the pressure and viscous effects exerted on the hydrofoil by the flowing water.

$$F_L = C_L \times \frac{1}{2} \times \rho \times A_s \times v^2 \quad (4)$$

The force exerted by the flowing water on the hydrofoil in the direction of the flow is known as drag or drag force. This drag force is always at right angle to the lift force. Drag is generated as a result of pressure and friction.

$$F_D = C_D \times \frac{1}{2} \times \rho \times A_s \times v^2 \quad (5)$$

These lift and drag forces have their own normal and tangential components and by summing these normal and tangential components the net normal and tangential forces are found. The tangential force is responsible for generating torque.

$$F_T = F_L \times (sin\alpha) - F_D \times (cos\alpha) \quad (6)$$

The normal force acting on the turbine blade orthogonal to the tangential force is:

$$F_N = F_L \times (cos\alpha) + F_D \times (sin\alpha) \quad (7)$$

The straight line connecting the leading and the trailing edge of the wing hydrofoil is known as chord and the angle formed between the relative velocity and chord is known as angle of attack.

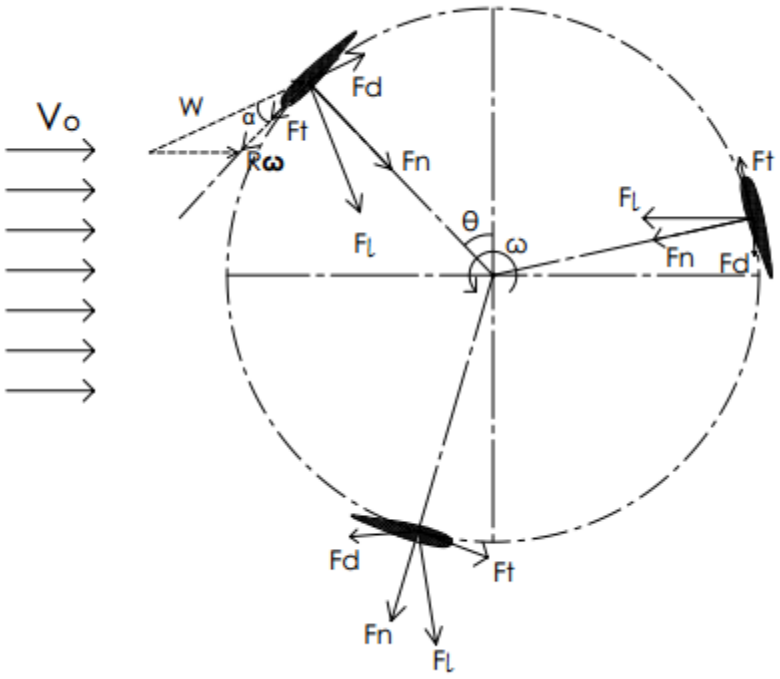

Figure 6: Forces acting on the rotor blades

The lift force is mainly dependent on the pressure differences across the hydrofoil surfaces whereas the drag force is mainly the sum of frictional drag (skin friction) and pressure drag. The values for both the drag coefficients vary with the AOA. In lift type devices, it is required that the hydrofoils must be designed such that they possess a higher lift coefficient and a lower drag coefficient.

Following are the are two important factors which play a vital role in determining the overall performance of the turbine:

1. Coefficient of Performance
2. Tip Speed Ratio

Coefficient of Performance:

The coefficient of performance is also known as the power coefficient of the turbine. It is defined as the ratio of the energy extracted by the turbine blades to the power available [5].

$$C_P = \frac{P_T}{P_A} \tag{8}$$

The available energy in flowing water is given by:

$$P_A = \frac{1}{2} \times \rho \times A_s \times v^3 \tag{9}$$

So the energy extracted by the rotor is then:

$$P_T = C_P \times \frac{1}{2} \times \rho \times A_s \times v^3 \tag{10}$$

Tip Speed Ratio:

Tip speed ratio is defined as the ratio of the speed of tip of blade (tangential speed) to the speed of incoming water flow [5].

$$\lambda = \frac{\omega \times R}{v_{in}} \tag{11}$$

3.2 Aerodynamic Model:

There are four primary models in order to study the performance of a crossflow (vertical axis) wind turbine [40].

Momentum Models

Vortex Models

Local Circulation Models

Viscous Models using CFD

Every model has its own strong and weak areas but the main attribute of momentum model is that its computational time is much less than the others. As far as CFD is concerned it takes too long for mesh generation in 3D analysis. We have used the

momentum models approach and the model is specifically defined as DMSV (Double Multiple Stream Tube) with variable interference factor based on the law of conservation of momentum. DMSV is hereby used in order to predict the overall torque produced by the Darrieus turbine rotor and thrust loads.
This model divides the rotor flow in two sections i.e. an upstream flow and a downstream flow. The actuator disk theory is used separately for both the upstream and the downstream part of the rotor.

Actuator Disc Theory:

This theory defines turbine as a disc which has a considerable pressure gradient across it. This pressure gradient is commonly known as pressure discontinuity and due to its presence the flow decelerates generating an induced velocity.

The volume of the flow enclosed by the rotor of turbine is known as its swept volume. DMSV divides this swept volume into a number of streamlines. These streamlines are assumed to be aerodynamically independent and are defined by their middle angles. The middle angle of a streamline is the angle between its position in the rotor and direction of free stream velocity. In analyzing the flow conditions each streamline is studied independently in the light of momentum and blade element theories. The momentum theory is based on the principle of conservation of angular and linear momentum whereas the blade element theory analyzes the forces acting on the blades (lift force and drag force) by dividing the blades into a number of elements.

It is assumed that the velocity of incoming flow decelerates near the turbine rotor. To break it down into two parts, the turbine is represented by two discs, one for the front turbine part and other for the rear one. Now the velocity decreases two times, at first for the upstream and then for the downstream. It is also assumed that there exists no change in the incoming flow velocity in the vertical direction and the rotor of the H-Darrieus turbine is subjected to constant flow velocity along its length.

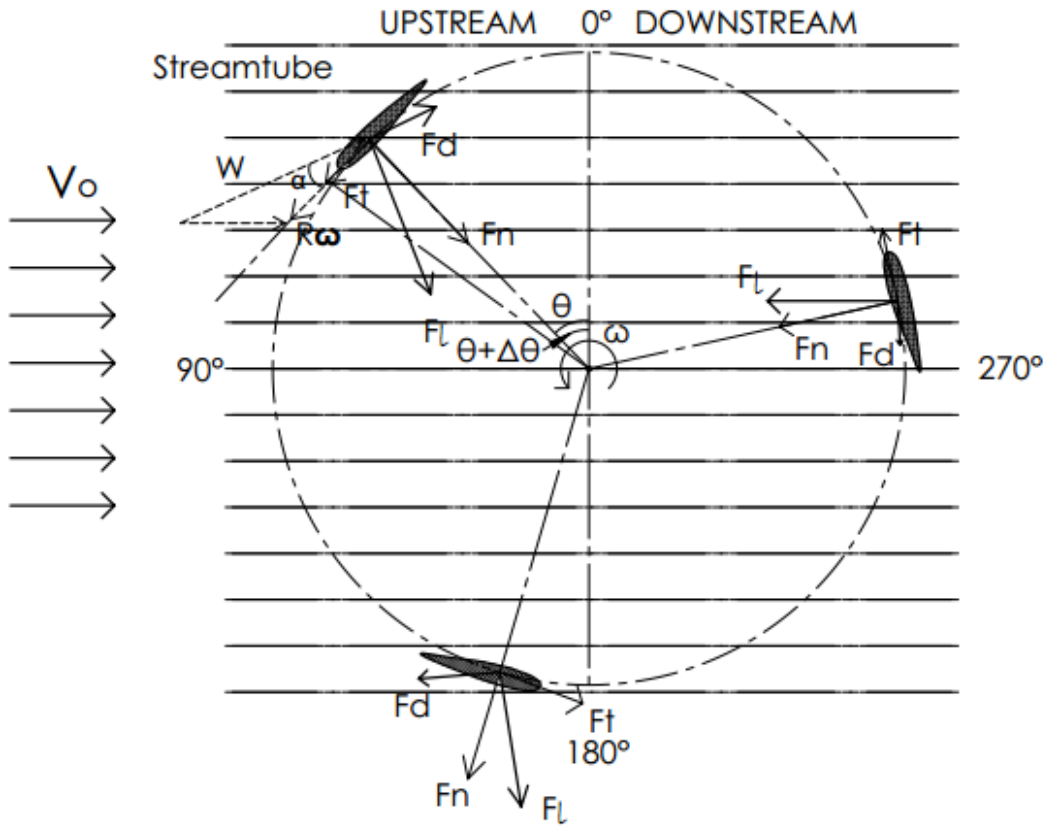

Figure 7: Division of rotor area into streamtubes

The induced velocity decreases in the flow direction in steps, such as the velocity in the upstream part of the rotor is represented by the following relation:

$$V_u = V_o \times a_u \tag{12}$$

In the above equation, V_o is the free flow velocity, a_u is the interference factor and the upstream induced velocity is represented by V_u. Now, coming towards the middle plane between the upstream and the downstream there exists a velocity known as equilibrium induced velocity represented by V_e such that:

$$V_e = V_o \times (2a_u - 1) \tag{13}$$

Likewise, the velocity for the downstream part of the rotor (V_d) is represented as follows:

$$V_d = V_e \times a_d \tag{14}$$

Here a_d is the downstream interference factor. Note that a_u is always greater than the a_d. The overall torque and coefficient of performance of the turbine rotor is dependent on the lift and drag forces and in order to calculate these forces at every position it is crucial to know the induced velocities everywhere around the trajectory of the rotor blade.

Depending upon the local tip speed ratio and the induced velocity, the resultant flow velocity can be evaluated by the following relation:

$$W_u = \sqrt{{V_u}^2 \times [(TSR - sin^2\theta)^2 + (cos^2\theta)]} \tag{15}$$

In the above equation, the resultant flow velocity is represented by W_u and TSR represents the local tip speed ratio.

$$TSR = R \times \frac{\omega}{V_u} \tag{16}$$

Here, rotor radius is represented by 'R' and the angular speed of the rotor is represented by ω. Now the local Reynolds number of the blade is determined using the resultant angular velocity.

$$Re_b = \frac{W_u \times c}{K_v} \tag{17}$$

Here Re_b represents the local Reynolds number and K_v is the kinematic viscosity. The following equation is used for predicting the angle of attack (α).

$$\alpha = \arcsin\left(\frac{cos\theta \times cos\alpha_o - (X - sin\theta) \times sin\alpha_o}{\sqrt{[(TSR - sin^2\theta)^2 + (cos^2\theta)]}}\right) \tag{18}$$

In above equation θ is the azimuth angle while α_o is the initial angle of attack. In the first half of the rotor which is known as the upstream part, the angle of attack is taken as a positive value because of the fact that the direction of relative wind speed vector is

outside the rotor periphery. The following relations are utilized in order to calculate the angle of attack at every position of the rotor blade:

$$\alpha_{right-half} = \arctan\left(\frac{V_u \times cos\theta}{(\omega \times R) + (V_u \times sin\theta)}\right) \quad (19)$$

$$\alpha_{left-half} = \arctan\left(\frac{V_u \times cos\theta}{(\omega \times R) - (V_u \times sin\theta)}\right) \quad (20)$$

In order to account for the coefficients of lift and drag, the local Reynolds number is used along with the angle of attack using the process of double interpolation. As the name suggests, in this process interpolation is done twice, once for Reynolds number and then again for the angle of attack.

By increasing the tsr the range of AOA decreases; as represented by the following figure:

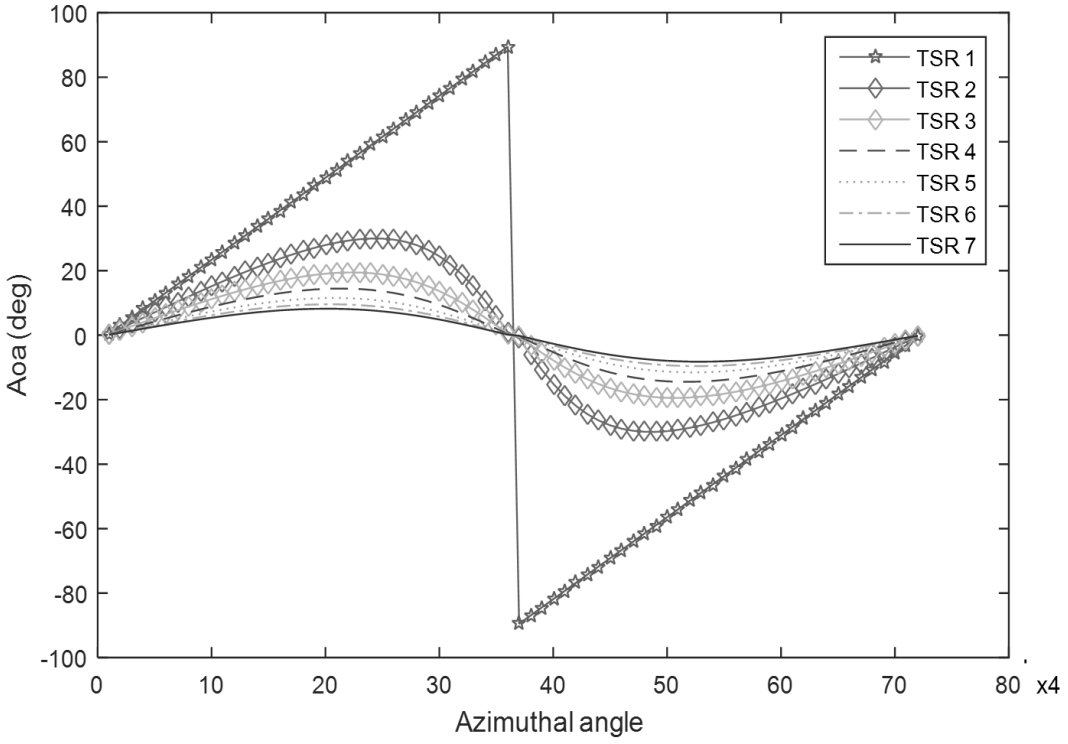

Figure 8: Graph of azimuthal angle vs AOA at different tip speed ratios.

The lift and drag forces are split into their normal and tangential components for predicting the torque output of the turbine. The corresponding coefficients of normal and tangential forces are evaluated by using the following relations:

$$C_N = C_L \times cos\alpha + C_D \times sin\alpha \tag{21}$$

$$C_T = C_L \times sin\alpha - C_D \times cos\alpha \tag{22}$$

In the above relations, C_N, C_T, C_L and C_D are the normal, tangential, lift and drag coefficients respectively. The interference factor is represented by the following equation:

$$a_u = \frac{\pi}{fup + \pi} \tag{23}$$

Where fup is a constant which characterizes the upstream flow conditions, such that:

$$fup = \frac{N \times c}{8 \times \pi \times R} \int_{-\frac{\pi}{2}}^{+\frac{\pi}{2}} |\sec\theta| \times (C_N \times \cos\theta - C_T \times \sin\theta)\, d\theta \tag{24}$$

Iteration Procedure:

Using equations from 12 to 24 for a given rotor geometry, rpm and free stream velocity of incoming flow, a first iteration is carried out using $a_u = 1$ and a new value for a_u is achieved. Now, with the new value of a_u the same iterative process is repeated until the initial and final values of a_u become similar. This process is repeated for each streamtube position and after evaluating all the induced upstream velocities the same procedure is repeated for the downstream half of the turbine rotor by substituting the upstream induced velocity with the downstream induced velocity [40].

Prediction of torque and overall performance:

Just like the lift and drag forces depend upon the lift and drag coefficient, the normal and tangential forces depend on the normal and tangential coefficients.

$$F_N(\theta) = \frac{1}{2} \times \rho \times c \times L \times W^2 \times C_N \tag{25}$$

$$F_T(\theta) = \frac{1}{2} \times \rho \times c \times L \times W^2 \times C_T \tag{26}$$

F_N and F_T are the normal and tangential forces respectively. W is the relative flow speed and L is the blade length. The overall torque produced by the blade is calculated as follows:

$$T(\theta) = \frac{1}{2} \times \rho \times c \times R \times L \times W^2 \times C_T \tag{27}$$

Whereas the average torque produced by the first half of the rotor (for upstream side using N/2 blades) is calculated by averaging the contributions of all the streamlines as follows:

$$T_{av} = \frac{N}{2\pi} \int_{-\frac{\pi}{2}}^{+\frac{\pi}{2}} T(\theta)\, d\theta \tag{28}$$

The average torque coefficient is calculated as follows:

$$Ct_{av} = \frac{T_{av}}{\frac{1}{2} \times \rho \times {V_O}^2 \times A_s \times R} \tag{29}$$

Now with the aid of average torque coefficient, the power coefficient for the upstream part is calculated as follows:

$$Cpu = Ct_{av} \times \lambda \tag{30}$$

Using the same equations from 27 to 30, the same procedure is repeated for the downstream part thus the torque (average) and the power coefficient for the downstream part is calculated. The overall value for the coefficient of performance or power coefficient is calculated by summing the two power coefficients of upstream and downstream part of the rotor. Therefore;

$$C_P = Cpu + Cpd \tag{31}$$

Where C_P is the total power coefficient and Cpd is the power coefficient of the downstream part of the rotor.

3.3 Limitations:

- As the flow velocity decreases it results in the expansion of the flow but DMSV does not account for the expansion of flow. The expansion of the flow effects the interference factor and its significance is higher at higher tip speed ratios. In our case the flowing fluid is water which is relatively less compressible than air therefore it can be termed as incompressible.
- DMSV doesn't incorporate the condition of dynamic stall. Aerodynamically, it is an unstable condition which occurs at low tsr as a result of large variations of AOA giving rise to vortex formation at the leading edge of the blade hydrofoil. As compare to static stall, relatively higher lift, drag and pitch moment coefficients are generated due these vortices.

3.4 Algorithm:

In order to perform the iterations and to plot the results a MATLAB algorithm was developed which is included in appendix 1.

The algorithm takes the rotor design parameters, free stream velocity as inputs. It is linked with a software known as "XFOIL" in order to read the corresponding hydrofoil coefficients of lift and drag depending upon the AOA and Reynolds number. An interference factor, relative water velocity, Reynolds number, AOA and tangential and normal forces are computed for every streamline.

A total of 36 streamlines were used for the above explained process which means predicting the conditions at every 5° increment.

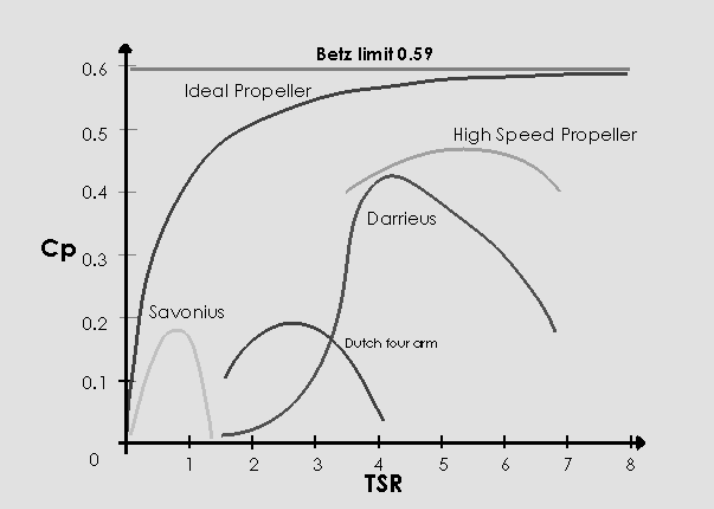

Figure 9: Power Coefficients vs Tip Speed Ratio

CHAPTER 4: RESULTS AND DISCUSSIONS

4.1 Results from MATLAB Algorithm:

It was found that the three hydrofoils were used commonly in different research papers which include NACA0012, NACA0015 and NACA0018. All of them are symmetric and have no camber profile. Using the MATLAB algorithm, we generated Cp vs tsr graphs, by using these three hydrofoils with different number of blades and varying solidity values for every number of blades. The number of blades tested were 2, 3 and 4 for each hydrofoil. In total, iterations were run for 9 different cases and Cp vs tsr graphs were obtained with varying solidity values as shown below from figure 10 till 18.

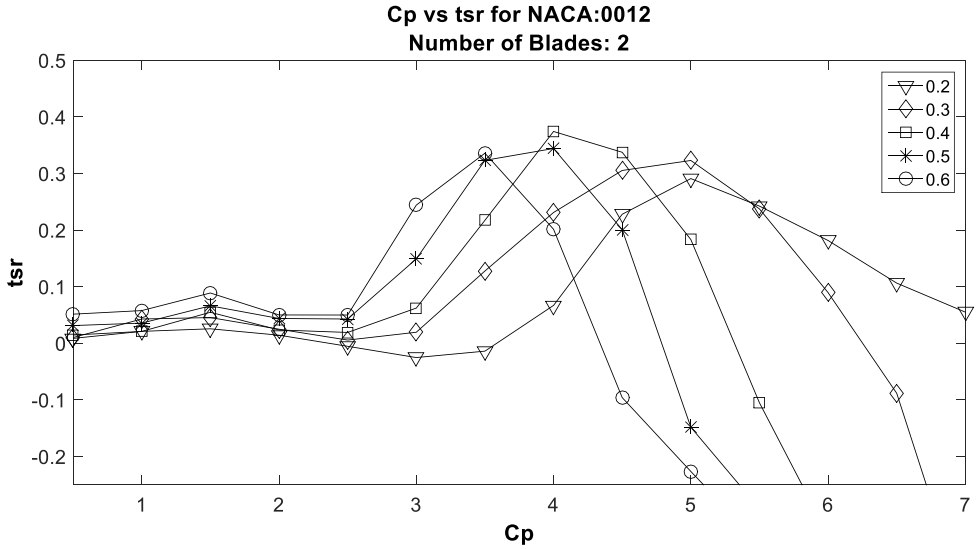

Figure 10: Cp vs tsr for N=2 - NACA0012 for different solidity values

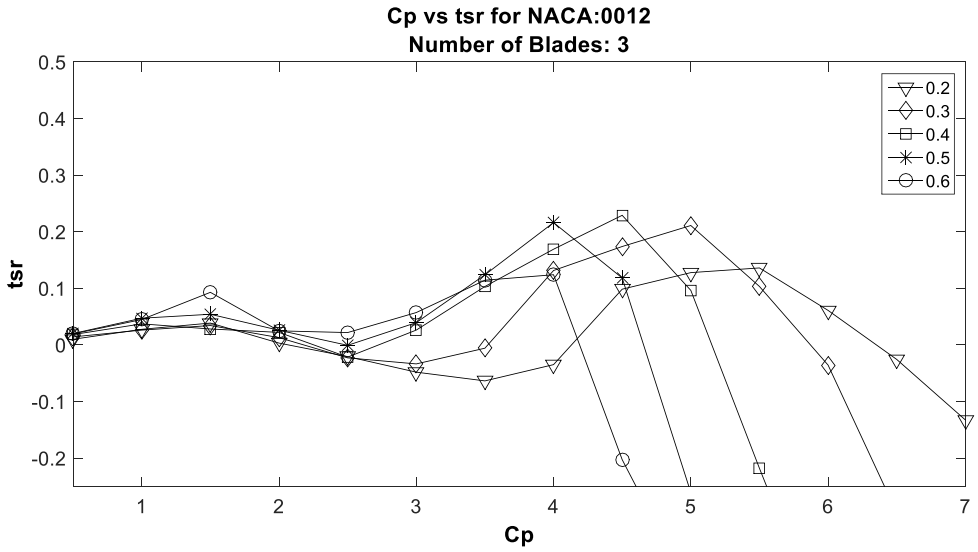

Figure 11: Cp vs tsr for N=3 - NACA0012 for different solidity values

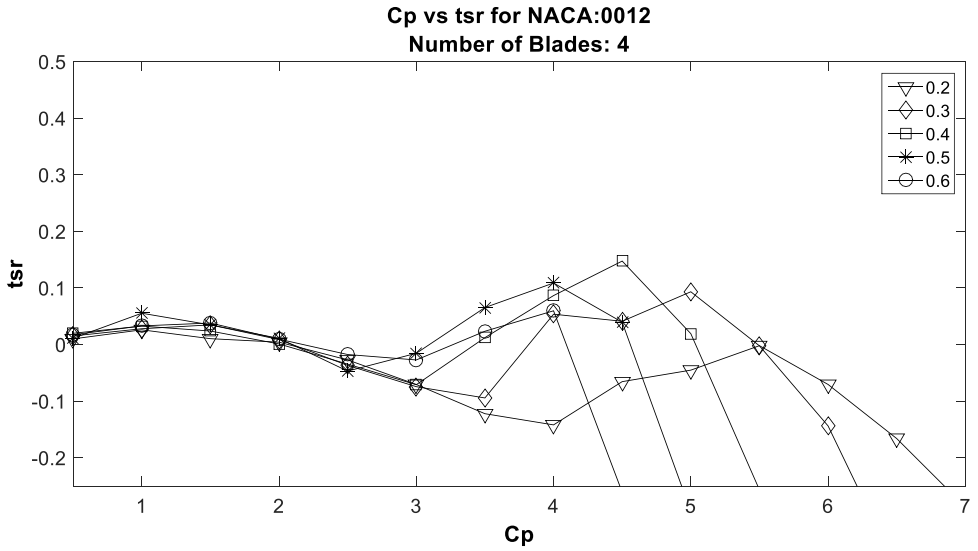

Figure 12: Cp vs tsr for N=4 - NACA0012 for different solidity values

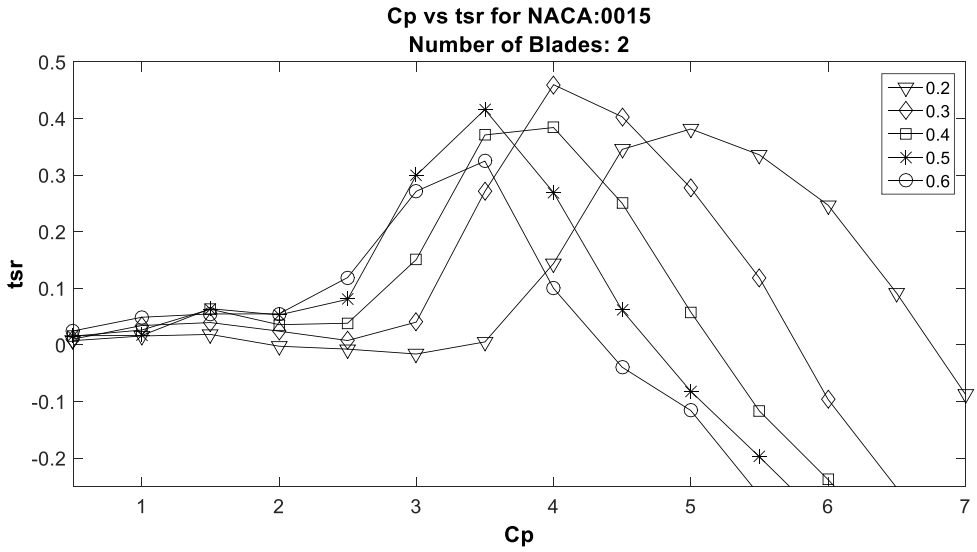

Figure 13: Cp vs tsr for N=2 - NACA0015 for different solidity values

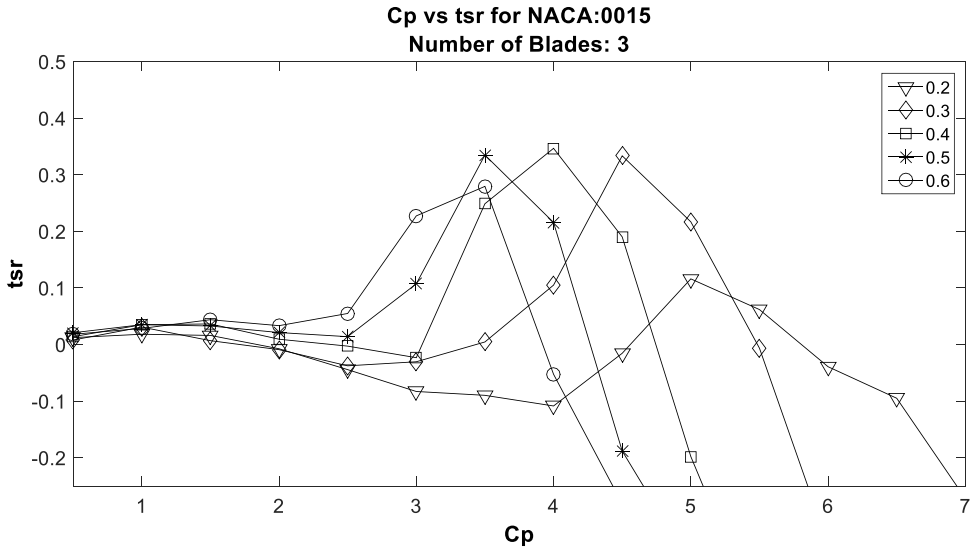

Figure 14: Cp vs tsr for N=3 - NACA0015 for different solidity values

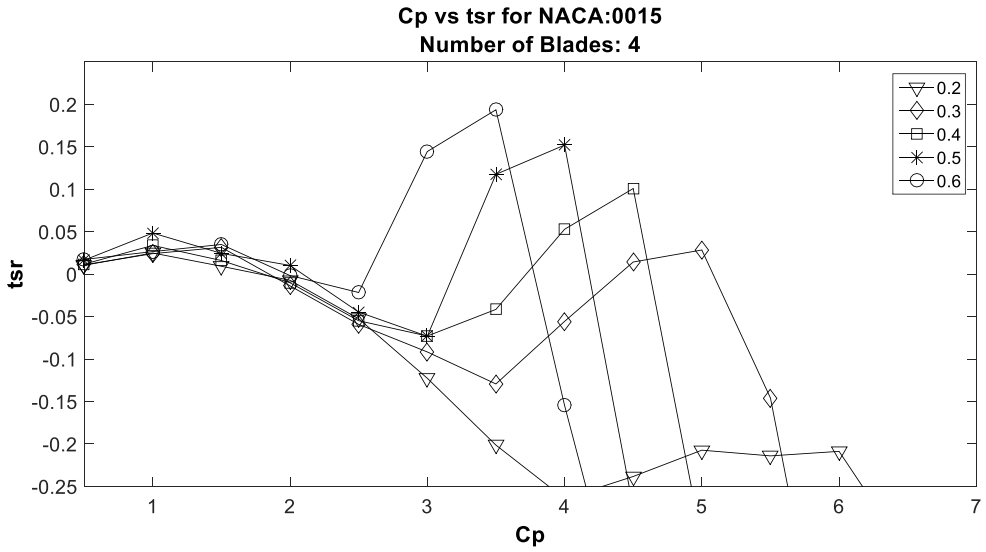

Figure 15: Cp vs tsr for N=4 - NACA0015 for different solidity values

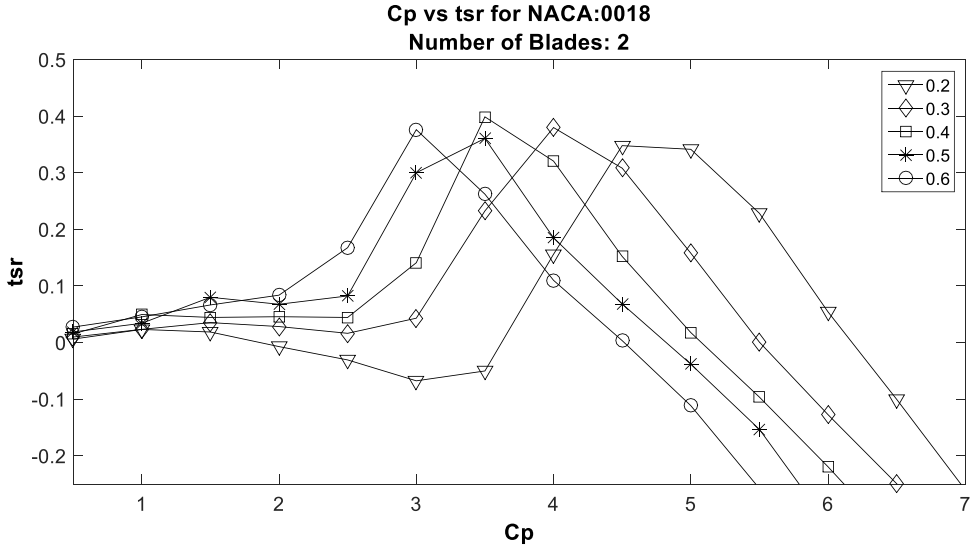

Figure 16: Cp vs tsr for N=2 - NACA0018 for different solidity values

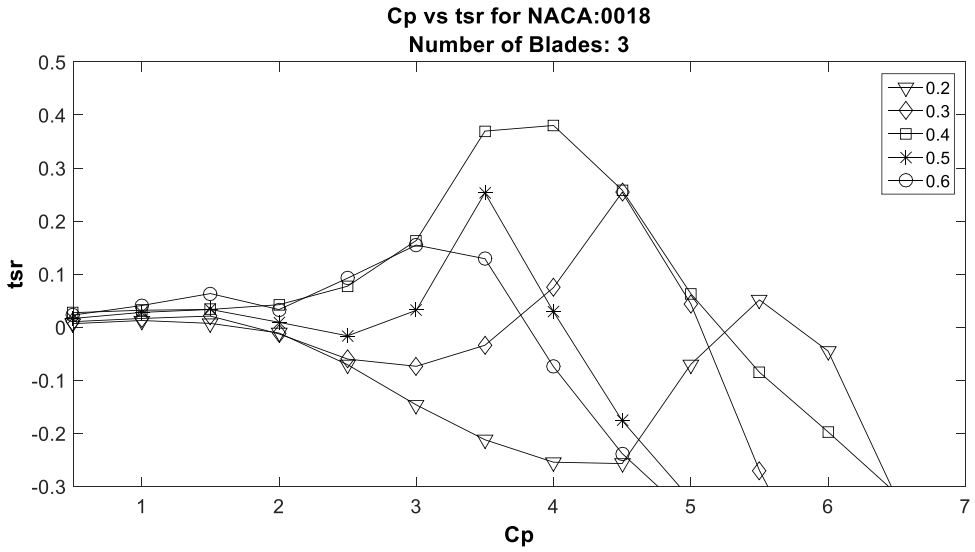

Figure 17: Cp vs tsr for N=3 - NACA0018 for different solidity values

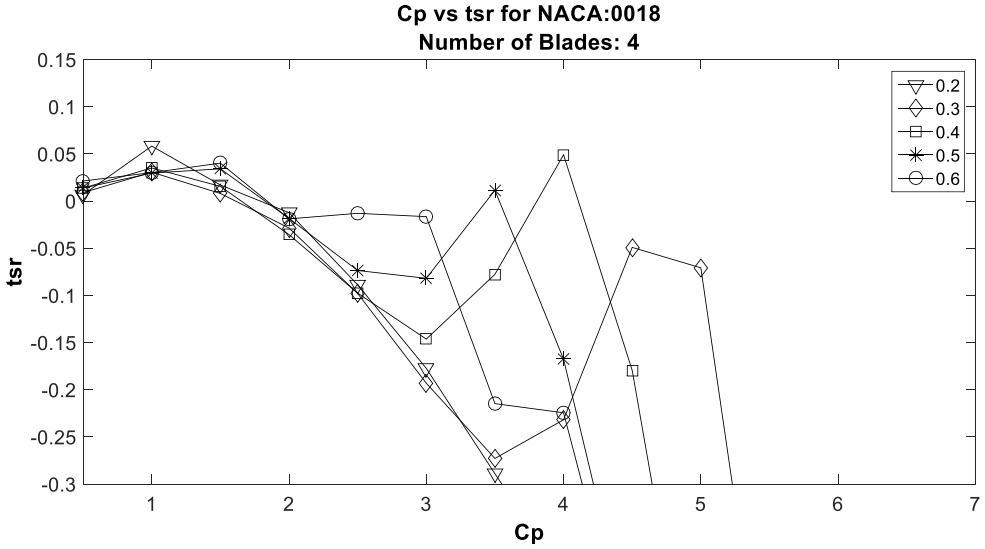

Figure 18: Cp vs tsr for N=4 - NACA0018 for different solidity values

It was found that the NACA0018, with 3 number of blades, having a solidity value of 0.4 showed maximum value for Cp i.e. 0.3802 at a tsr value of 4.0.

4.2 Material Selection:

This section is divided into two phases. In the first phase, theoretical calculations would be used to predict the material for the turbine whereas in the second phase a model of turbine would be developed in SOLIDWORKS and its finite element analysis would be done in ANSYS. The forces that are used in ANSYS was calculated from DMST theory. This analysis would be helpful in acquiring stresses and strain values and these can be used to determine the material for the turbine.

Procedure

In vertical axis turbines we are using aerodynamic shape blades. In our case it is NACA 0012 blade. The co-efficient of lift and drag at different angles of attack are given in literature and also can be found from XFOIL, XFLR or Q-Blade software at different Reynold number. These values are than used in DMST to find tangential and normal forces on blades that we used in our FEM analysis.

Finite element method is an essential analysis technique which helped us in assessing the design parameters of a turbine. We used FEM to find Von Mises stress, normal stress, shear stress and the factor of safety, given that initially we selected a material for comparison with its yield strength. In the end, the apt material is proposed which would withstand the normal and tangential components of aerodynamic forces.

4.3 Theory or Analytical Results

Bending of Hydrofoil blade

In order to find the maximum deflection on the hydrofoil blade due to normal aerodynamic forces, it can be analyzed as a beam with fixed support at radial arms having a uniformly distributed loading.

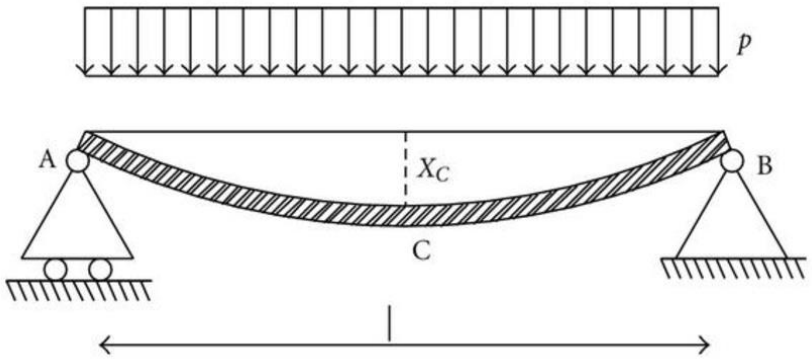

Figure 19: Deflection in a beam

Since,

F_N= 1.1 N,

F_T=0.1102 N

And height of aerofoil blade H_B= 40 cm

Here p is the uniformly distributed loading on the blade and is:

$$P = F_N/H_B = 2.75 \text{ N/m} \tag{32}$$

Maximum deflection is given by:

$$X_C = \frac{5pH_B{}^4}{384\,EI} \tag{33}$$

Where E= 200GPa

Chord length of hydrofoil is 3.333 cm so for simplification it is assumed to be a rectangle of dimensions 3.333 cm x 40 cm

$$I = \frac{bd^3}{12} \tag{34}$$

where b= 3.333 cm and d= 3.85 x 10^{-3} m

I=1.58 x 10^{-10} m^4

X_C = 0.029 mm

This shows that maximum deflection in hydrofoil has an insignificant effect on bending.

This rectangular beam is indeterminate since it has two fixed supports. In order to solve the beam, we used the method of fixed end moments. In this method, horizontal reactions are neglected. In order to calculate vertical reactions, we analysed the beam as a simply supported beam. For moments, we used fixed end moments method which is shown below for point loads and uniformly distributed load.

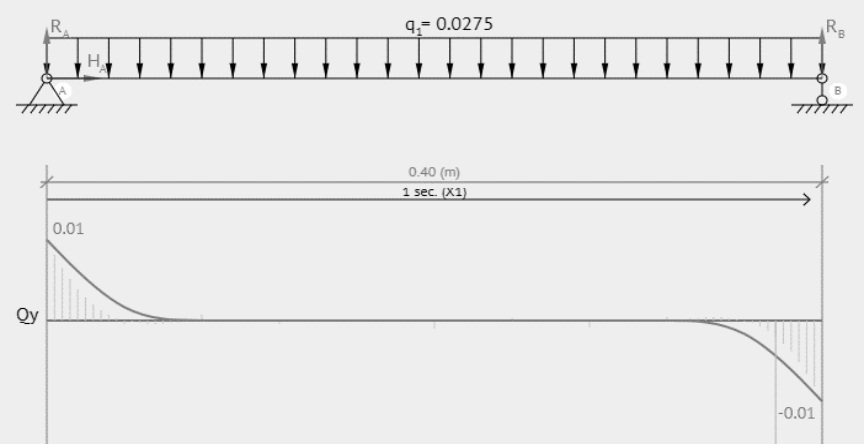

Figure 20: Shear force Bending Moment diagram

For equilibrium:

$\Sigma F_X = 0$: $H_A = 0$

$\Sigma M_A = 0$: The sum of the moments about a point A is zero:

$$-\,q1 * 0.4 * (0.4/2) \;+\; RB * 0.4 \;=\; 0 \qquad (35)$$

$\Sigma M_B = 0$: The sum of the moments about a point B is zero:

$$-\,RA * 0.4 \;+\; q1 * 0.4 * (0.4 \;-\; 0.4/2) \;=\; 0 \qquad (36)$$

Solving this system of equations:

$H_A = 0$ (N)

Calculate reaction of roller support about point B:

$$\text{RB} = (0.0275 * 0.4 * (0.4/2)) / \mathbf{0.4} = 0.0137 \text{ (N)} \quad (37)$$

Calculate reaction of pin support about point A:

$$\text{RA} = (0.0275 * 0.4 * (0.4 - 0.4/2)) / \mathbf{0.4} = 0.0137 \text{ (N)} \quad (38)$$

Moment can be calculated through fixed end moment:

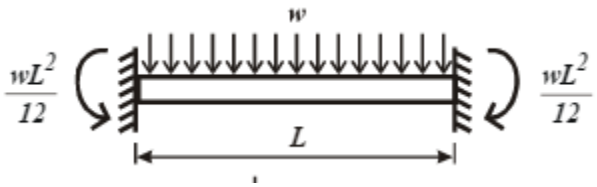

Figure 21: Fixed beam with uniformly distributed load

$$\text{M} = \frac{wL^2}{12} = 0.00275\text{x}\frac{0.42}{12} = 0.000037 \text{ kNm} \quad (39)$$

We calculated the bending stress using flexure formula:

$$\sigma = \frac{M_{max} \times c}{I_{XX}} \quad (40)$$

where c= 1.925 x 10^{-3}

I_{XX}= 1.58 x 10^{-10} m^4

σ=0.45 MPa << σ_Y

We calculated maximum shear stress using:

$$\tau = \frac{V_{max} \times Q_{max}}{I \times t} \quad (41)$$

V_{MAX}= 0.0137 KN

t=0.3333 m

$$Q_{MAX} = y \times A = 1.23397 \text{ x } 10^{-7} \text{ m}^3 \quad (42)$$

Hence τ = 0.32 MPa << τ_Y

Our design is well within the safety limit.

Bending in the tangential direction would be insignificant since $F_T << F_N$.

Radial arm compression:

Radial arms are in compression due to normal aerodynamic force so buckling can be analysed on it using both fixed supports at the end. Since there are two radial arms, it is assumed that normal force is divided among both arms.

$F= F_N/2$

F=0.55 N

E=200 GPa

$$I = \frac{bd^3}{12} \tag{43}$$

where b= 8 mm and d= 3.25 mm

A= 8 x 3.25 = 26 x 10^{-6} m^2

I=22.885 x10^{-12} m^4

Length of radial arm H = 0.4 m

For buckling:

$$P_{cr} = \frac{\pi \times E \times I}{(K \times H)^2} \tag{44}$$

Where K= 0.5 for both fixed ends

P_{CR}=1129.65 N > F therefore yielding will occur before buckling.

$$\sigma = \frac{F}{A} \tag{45}$$

σ = 21 k Pa therefore any material having yield stress greater than this multiplied by factor of safety times can be selected to ensure that radial arm will not deform plastically.

Radial arm bending:

In order to find bending on radial arm, it is assumed that tangential force is solely acting on the radial arm and the central shaft is fixed whereas the other end of arm is free, so the arm acts as a cantilever beam.

F= $F_T/2$ = 0.05501 N

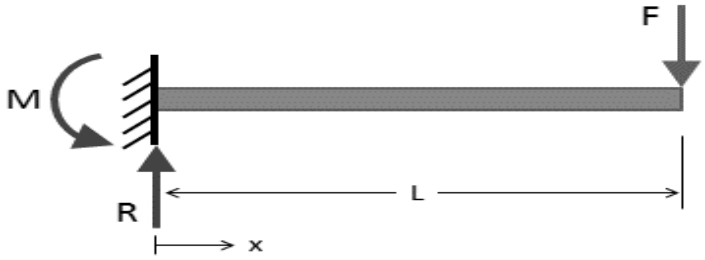

Figure 22: Cantilever beam with fixed support

Maximum deflection at the end is given by:

$$\delta_{end} = \frac{Fl^3}{3EI} \tag{46}$$

E=200 GPa

I=22.885 x10^{-12} m^4

L = 0.2 m

$$\boldsymbol{\delta_{end} = 0.0321\ mm}$$

This shows that maximum deflection in radial arm has an insignificant effect on bending.

Torsional stress in shaft:

Torque of the shaft can be calculated by:

$$T = 3 \times F_T \times R \quad (47)$$

where 3 is the number of blades

Radius of turbine R =0.4 m

T = 0.13224 Nm

In the worst-case scenario of generator's rotor stuck due to any issue, we will be calculating angle of twist of shaft through:

$$\emptyset = \frac{TL}{JG} \quad (48)$$

Where L is distance of shaft from the bottom to its transmission to the generator to the top

L=0.6 m

J is polar moment of inertia of shaft and is given by:

$$J = \frac{\pi}{32} D^4 \quad (49)$$

Where d is the diameter of shaft and is:

D = .014 m

J=0.37 x 10^{-9} m^4

G= 7.69 x 10^{10} Pa

Hence $\emptyset = 0.00279$ radians

OR $\emptyset = 0.159\ °$

Angle of twist indicates that shear stress in the shaft would be low even in the worst-case scenario.

4.4 Geometric Model:

Dimensions:

Table 2: Dimensions

Chord length	3.33 cm
Height of turbine blade	40 cm
Diameter of shaft	14 mm
Radius of turbine	40 cm
Dimensions of radial arm	8 by 3.25 mm

4.5 Finite Element Model

Geometry:

SOLIDWORKS was used to form 3D model of turbine. The model was then converted to step file as a single body and was import in ANSYS for analysis. The model contains NACA 0012 hydrofoil shape blades, radial arms and a central shaft. Aerodynamic forces were calculated using DMST[40] theory and from these values tangential and normal forces of blades were calculated and used in ANSYS.

Meshing:

The model contains hydrofoil shapes which have curvature, so in mesh we turned on advance size function to curvature and set relevance centre to fine.

The final meshed model is as shown below.

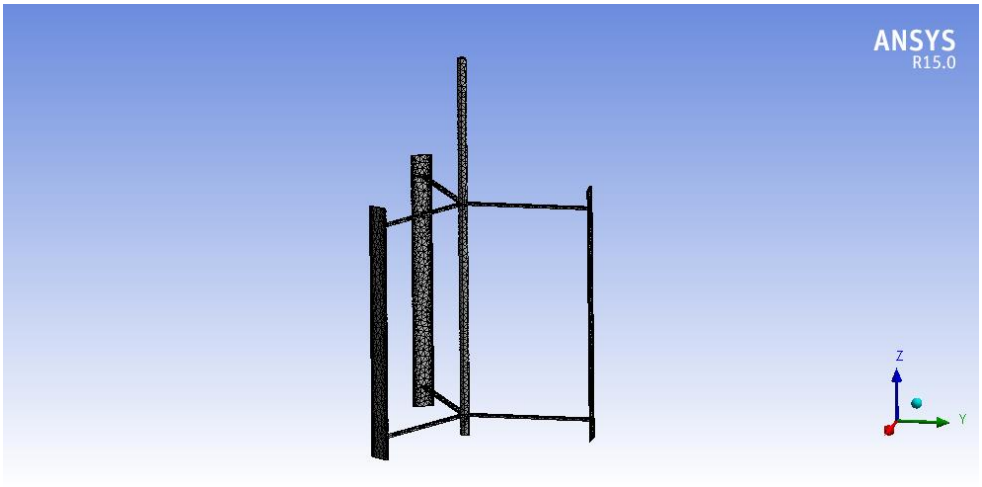

Figure 23: Meshed Model

Analysis:

Aerodynamic forces were calculated using DMST theory and from these values tangential and normal forces of blades were calculated and used in ANSYS. Tangential force was calculated to be 0.1102 N and normal force was calculated to be 1.1 N. these forces were applied on each blade. There were 6 forces in total, 3 tangential and 3 normal and one support at generator connection which was assumed to be fixed as a worst-case scenario at max load. All forces are shown on model are shown below.

Total deformation:

Max deformation was 0.025753mm.

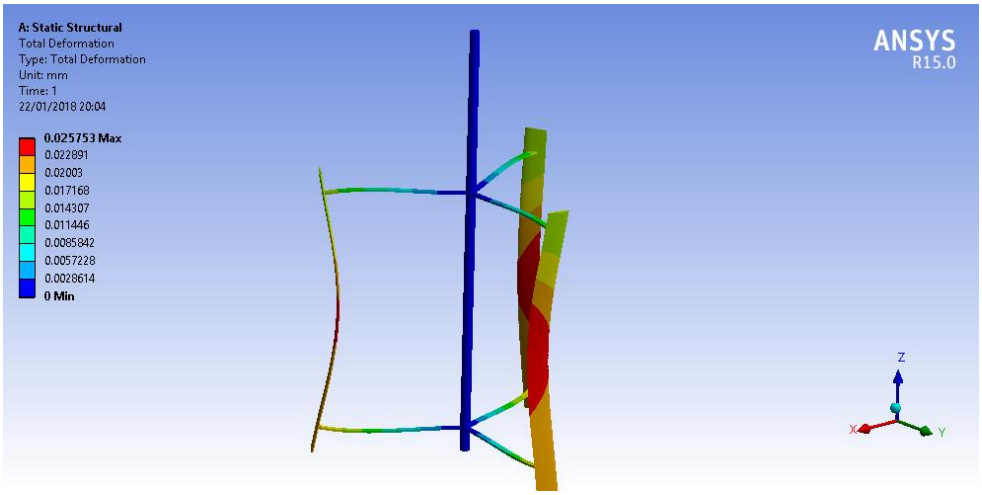

Figure 24: Total Deformation

Normal Stress:

Max normal stress was found to be 0.62175 MPa at radial arm

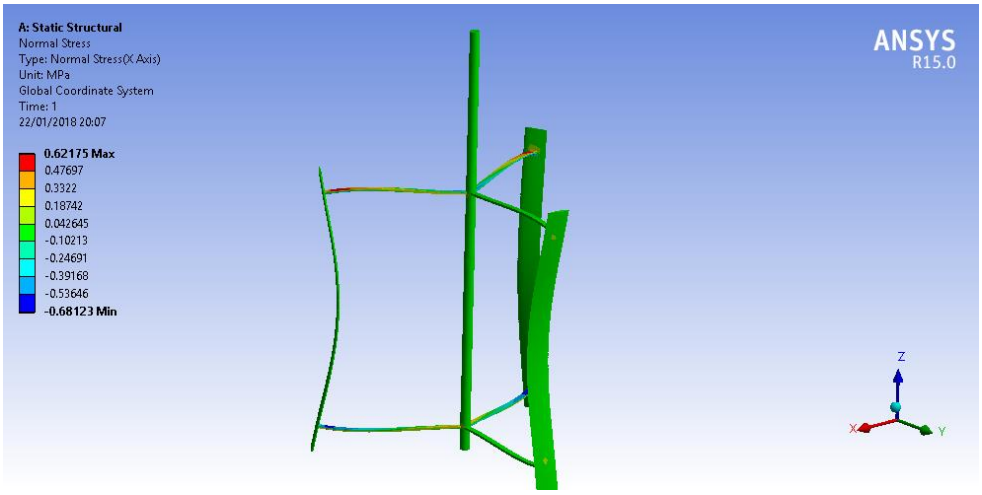

Figure 25: Normal Stress

Shear stress:

Max Shear stress is 0.34764 MPa at radial arm.

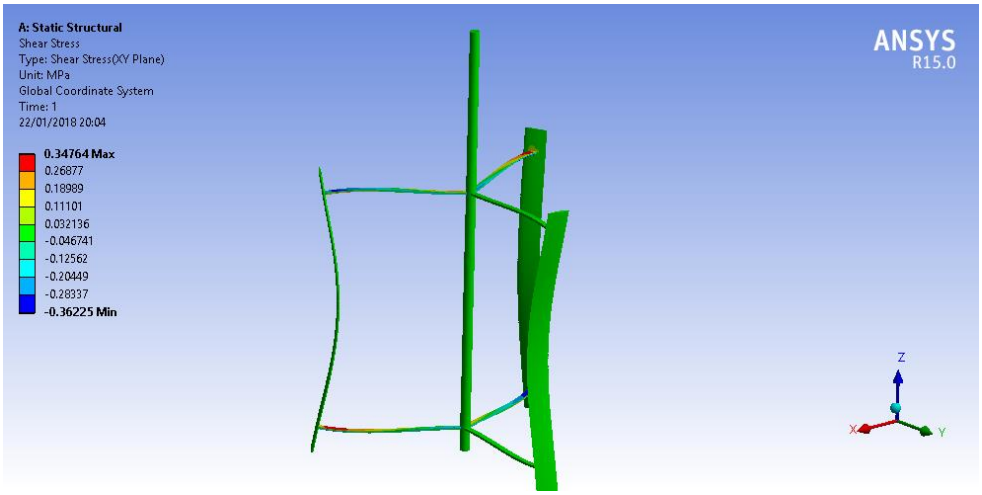

Figure 26: Shear Stress

Equivalent Stress:

Max equivalent (Von-Mises) was found out to be 0.85535 MPa.

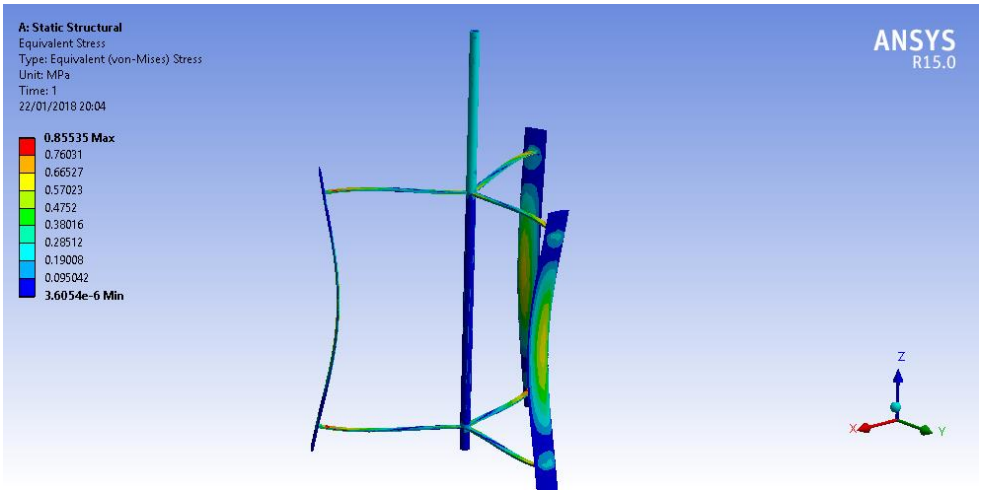

Figure 27 *Equivalent Stress Von-Misses*

Factor of Safety:

FOS of whole model was found to be 15, which shows under given conditions and material, model is safe.

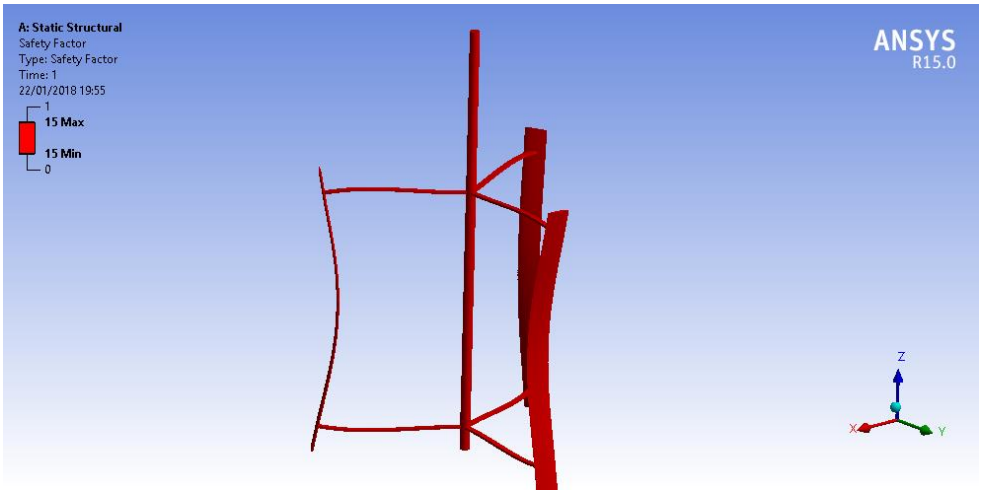

Figure 28: Factor of Safety

4.6 Results:

Testing was performed in water tunnel with different combinations of Darrieus and Savonius. Each combination was tested on two different flowrates by varying the frequency of pump. We had two different sizes of three Darrieus blades categorized as small and large, one two bladed Savonius and one three bladed Savonius. We tested seven combinations for one flowrate, so in total we performed fourteen experiments. In each experiment we measured breaking torque. The results were very conclusive and, in the end, we found one suitable combination.

Breaking Torque Setup:

A moment arm was fixed to turbine shaft and in the front of that moment arm we had a load cell that was fixed on the platform. We took multiple values of torque for each combination and averaged them to get the value breaking torque for that combination. Length of moment arm was suitable enough to get measurable reading on load cell. The sensitivity of load cell used was 1 g.

RPM measurements:

Tachometer was used to measure RPM of different combinations; however main focus was to study breaking torque for each combination.

Breaking Torque values for different combinations at Pump frequency 30 Hz:

Pump frequency 30 Hz correspond to almost 0.35 m/s flow velocity of water tunnel. See the figure below.

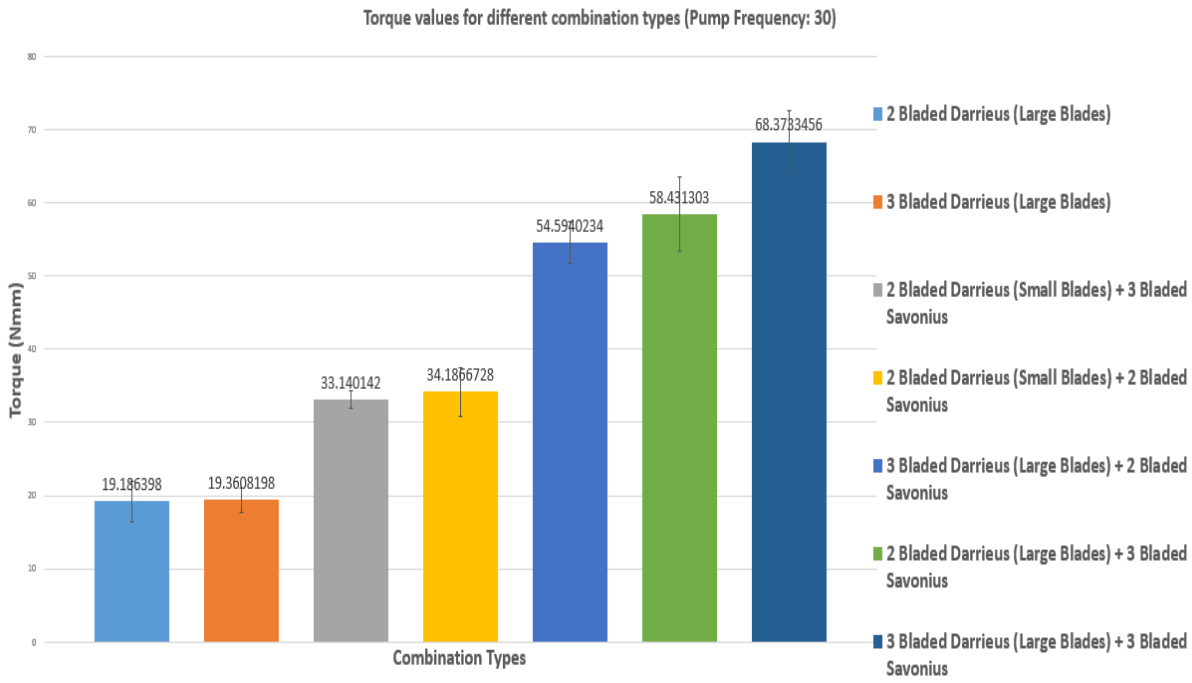

Figure 29: Breaking torque values at 0.3 m/s

Highest breaking torque was around 69 N-mm for three bladed large Darreius coupled with three bladed Savonius.

Breaking Torque values for different combinations at Pump frequency 35 Hz:

Pump frequency 30 Hz correspond to almost 0.4 m/s flow velocity of water tunnel. See the figure below. In this figure the highest value of breaking torque is around 70 N-mm which is also for three bladed large Darreius coupled with three bladed Savonius. So, the optimum combination found was three bladed large Darrieus coupled with three bladed Savonius.

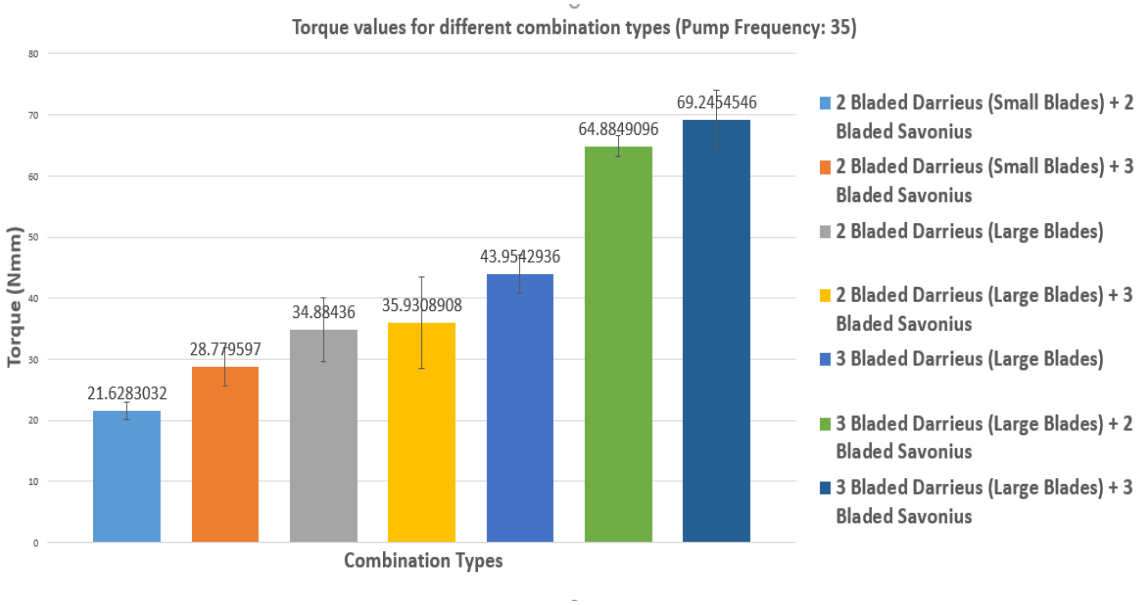

Figure 30: Breaking torque values at 0.4 m/s

CHAPTER 5: CONCLUSION AND RECOMMENDATION

The main objective of this project was to design a hybrid Darrieus Savonius hydrokinetic turbine. The advantage of hybrid design was a self-starting and a more efficient turbine than a single rotor. The method used to design Darrieus turbine was Double Multiple Stream tube model with the help MATLAB. DMST is a kind of iterative process in which we can obtain optimized values/ of all parameters for Darrieus turbine. The maximum power co-efficient obtained from DMST was 0.45 for two-bladed turbine. However, experiments showed that three-bladed are more practical than two-bladed turbine. The Savonius turbine was designed with the help of Computational Fluid Dynamic in ANSYS. Different overlap ratios and different number of blades for Savonius were studied to get an optimized design. The maximum co-efficient of performance for Savonius was found out to be 0.2.

The next phase of project was experimentation. The purpose of experimentation was to find a suitable combination for Darrieus and Savonius turbine. We had two different sizes of Darrieus blades, one two bladed Savonius and one three bladed Savonius. We tested multiple combinations to get an optimized combination in which we can get maximum efficiency.

From experiments it was concluded that the optimum combination is three bladed large Darrieus coupled with three bladed Savonius. It was also evident from the results that the value of breaking torque for the hybrid turbine is greater than breaking torque of individual turbine, which was the main objective of our study that hybrid turbines are

more efficient than individual turbine. The flowrates at which we tested our design were very low and meant only for the design purpose. The flow velocity at these flowrates was around 0.35 to 0.4 m/s, however in Canals we have flow velocity of around 1.5 m/s which is enough to generate power, as we have cube of velocity in power formula that is why the minimum flow velocity at which we can have considerable power generation is 1 m/s.

From results it was also concluded that a hybrid turbine of overall dimensions of 1x1 m of this design is large enough to produce 1 kW of power at flow velocity of 1.5 m/s. In Pakistan we are facing a major shortfall of electricity, this technology is very promising in overcoming the shortfall of electricity in rural areas of Pakistan where we also have Canals. By installing a hybrid turbine of 1 kW in a Canal we can easily provide sufficient power to one house in rural area.

The additional mooring mechanism is also to be designed for easy installation of these turbine which includes floating mechanism and ropes to anchor turbine in place.

For extracting individual power from each turbine, an epicyclic gear train is needed which was not scope of our project. However, to have this project in running phase, epicyclic gear train is also needed to be designed. In epicycle gear train we can have two input and resulting one output. The shaft of turbine to which Savonius is directly attached is connected to sun of epicyclic gear train and as the Darrieus is connected to shaft with help of freewheel, so the output from Darrieus turbine should be taken from freewheel

connected to ring of epicyclic gear train. The combined output is at the planet of epicyclic gear train which is to be connected to generator for power generation.

These hybrid hydrokinetic turbines can be used to produce power ranging from 1 kW to 50 kW depending on the size and configurations in remote area to overcome the shortfall of electricity. So, this project of hybrid hydrokinetic turbine opened a new area of research to develop more efficient turbines. Above all, this is also very clean and cheap source of producing electricity just from flowing water outside without any major civil work on hand. Beside canals, these turbines can also be placed in rivers and seas to provide electricity for offshore and onshore power requirements.

WORKS CITED

1. Khan, M., et al., *Performance of Savonius rotor as a water current turbine.* The Journal of Ocean Technology, 2009. **4**(2): p. 71-83.
2. Khan, M.J., et al., *Hydrokinetic energy conversion systems and assessment of horizontal and vertical axis turbines for river and tidal applications: A technology status review.* Applied Energy, 2009. **86**(10): p. 1823-1835.
3. Khan, M.J., M.T. Iqbal, and J.E. Quaicoe, *River current energy conversion systems: Progress, prospects and challenges.* Renewable and Sustainable Energy Reviews, 2008. **12**(8): p. 2177-2193.
4. Güney, M.S. and K. Kaygusuz, *Hydrokinetic energy conversion systems: A technology status review.* Renewable and Sustainable Energy Reviews, 2010. **14**(9): p. 2996-3004.
5. Kumar, A. and R.P. Saini, *Performance parameters of Savonius type hydrokinetic turbine – A Review.* Renewable and Sustainable Energy Reviews, 2016. **64**(Supplement C): p. 289-310.
6. Eriksson, S., H. Bernhoff, and M. Leijon, *Evaluation of different turbine concepts for wind power.* Renewable and Sustainable Energy Reviews, 2008. **12**(5): p. 1419-1434.
7. Baxter, R.M., *Environmental effects of reservoirs*, in *Microbial Processes in Reservoirs*, D. Gunnison, Editor. 1985, Springer Netherlands: Dordrecht. p. 1-26.
8. El-Shamy, F.M., *Environmental impacts of hydroelectric power plants.* J. Hydraul. Div., Am. Soc. Civ. Eng.;(United States), 1977. **103**.
9. Hoq, M.T., et al., *Micro hydro power: promising solution for off-grid renewable energy source.* Int. J. Sci. Eng. Res., 2011. **2**(12): p. 1-5.
10. Zhou, H., *Maximum power point tracking control of hydrokinetic turbine and low-speed high-thrust permanent magnet generator design*. 2012, MISSOURI UNIV OF SCIENCE AND TECHNOLOGY ROLLA.
11. Senat, J., *Numerical simulation and prediction of loads in marine current turbine full-scale rotor blades*. 2011: Florida Atlantic University.
12. Khan, M., et al., *Hydrokinetic energy conversion systems and assessment of horizontal and vertical axis turbines for river and tidal applications: A technology status review333.* Applied energy, 2009. **86**(10): p. 1823-1835.

13. Ginter, V.J. and J.K. Pieper, *Robust gain scheduled control of a hydrokinetic turbine.* IEEE Transactions on Control Systems Technology, 2011. **19**(4): p. 805-817.

14. Efficiency, U.S.D.o.E.O.o.E., et al., *Ocean Energy Technology Overview: Federal Energy Management Program (FEMP)*. 2009: United States. Department of Energy. Office of Energy Efficiency and Renewable Energy.

15. Kuschke, M. and K. Strunz. *Modeling of tidal energy conversion systems for smart grid operation*. in *Power and Energy Society General Meeting, 2011 IEEE*. 2011. IEEE.

16. Suprayogi, D.T., *Savonius rotor vertical axis marine current turbine for renewable energy application*. 2010, Universiti Teknologi Malaysia.

17. Adriane Prisco, P., V. Horcio Antonio, and A. Joo Vicente, *A review on the performance of Savonius wind turbines.* Renewable and Sustainable Energy Reviews, 2012.

18. Beri, H. and Y. Yao, *Double multiple streamtube model and numerical analysis of vertical axis wind turbine.* Energy and Power Engineering, 2011. **3**(03): p. 262.

19. Kamoji, M.A., S.B. Kedare, and S.V. Prabhu, *Experimental investigations on single stage, two stage and three stage conventional Savonius rotor.* International Journal of Energy Research, 2008. **32**(10): p. 877-895.

20. Vermaak, H.J., K. Kusakana, and S.P. Koko, *Status of micro-hydrokinetic river technology in rural applications: A review of literature.* Renewable and Sustainable Energy Reviews, 2014. **29**(Supplement C): p. 625-633.

21. Alexander, A. and B. Holownia, *Wind tunnel tests on a Savonius rotor.* Journal of Wind Engineering and Industrial Aerodynamics, 1978. **3**(4): p. 343-351.

22. Tong, W., *Wind power generation and wind turbine design*. 2010: WIT press.

23. Brusca, S., R. Lanzafame, and M. Messina, *Design of a vertical-axis wind turbine: how the aspect ratio affects the turbine's performance.* International Journal of Energy and Environmental Engineering, 2014. **5**(4): p. 333-340.

24. Vance, W. *Vertical axis wind rotors–status and potential*. in *Proceedings of the conference on wind energy conversion systems*. 1973.

25. Iio, S., et al., *Influence of setting condition on characteristics of Savonius hydraulic turbine with a shield plate 39.* Journal of Thermal Science, 2011. **20**(3): p. 224-228.

26. Kamoji, M., S. Kedare, and S. Prabhu, *Experimental investigations on single stage, two stage and three stage conventional Savonius rotor.* International journal of energy research, 2008. **32**(10): p. 877-895.

27. Saha, U., S. Thotla, and D. Maity, *Optimum design configuration of Savonius rotor through wind tunnel experiments 55.* Journal of Wind Engineering and Industrial Aerodynamics, 2008. **96**(8): p. 1359-1375.

28. Saha, U. and M.J. Rajkumar, *On the performance analysis of Savonius rotor with twisted blades 56.* Renewable energy, 2006. **31**(11): p. 1776-1788.

29. Nakajima, M., S. Iio, and T. Ikeda, *Performance of Savonius rotor for environmentally friendly hydraulic turbine 57.* Journal of Fluid Science and Technology, 2008. **3**(3): p. 420-429.

30. Nakajima, M., S. Iio, and T. Ikeda, *Performance of Savonius rotor for environmentally friendly hydraulic turbine 58.* Journal of Fluid Science and Technology, 2008. **3**(3): p. 420-429.

31. Mabrouki, I., Z. Driss, and M.S. Abid, *Performance Analysis of a Water Savonius Rotor: Effect of the Internal Overlap 59.* Sustainable Energy, 2014. **2**(4): p. 121-125.

32. Khan, M., et al., *Performance of Savonius rotor as a water current turbine 60.* The Journal of Ocean Technology, 2009. **4**(2): p. 71-83.

33. Grinspan, A. and U. Saha, *Experimental investigation of twisted bladed Savonius wind turbine rotor 61.* International Energy Journal, 2005. **5**.

34. Ghatage, S.V. and J.B. Joshi, *Optimisation of vertical axis wind turbine: CFD simulations and experimental measurements 62.* The Canadian Journal of Chemical Engineering, 2012. **90**(5): p. 1186-1201.

35. Damak, A., Z. Driss, and M. Abid, *Experimental investigation of helical Savonius rotor with a twist of 180 reference.* Renewable Energy, 2013. **52**: p. 136-142.

36. Sivasegaram, S., *Secondary parameters affecting the performance of resistance-type vertical-axis wind rotors.* Wind Engineering, 1978: p. 49-58.

37. Jeon, K.S., et al., *Effects of end plates with various shapes and sizes on helical Savonius wind turbines 66.* Renewable Energy, 2015. **79**: p. 167-176.

38. OGAWA, T. and H. YOSHIDA, *The effects of a deflecting plate and rotor end plates on performances of Savonius-type wind turbine 67.* Bulletin of JSME, 1986. **29**(253): p. 2115-2121.

39. Mahmoud, N., et al., *An experimental study on improvement of Savonius rotor performance 54.* Alexandria Engineering Journal, 2012. **51**(1): p. 19-25.

40. Paraschivoiu, I., *Wind Turbine Design: With Emphasis on Darrieus Concept*. 2002: Polytechnic International Press.

APPENDIX I: MATLAB CODE FOR DOUBLE MULTIPLE STREATUBE MODEL OF DARRIEUS ROTOR

Constants:

```
Kv=0.801*10^-6;                 %Kinematic viscosity of water
rho=1000;                       %Density of water
n=36;                           %Number of stream tubes
thetau=linspace(-89*pi/180,89*pi/180,n);%Dividing upstream theta into 36 points
thetad=linspace(91*pi/180,269*pi/180,n);%Dividing downstream theta into 36
points
V0=input('Enter Water Velocity ');
TSR=input('Enter TSR ');
S=input('Enter rotor area ');
AR=input('Enter aspect ratio(L/R) ');%Aspect Ratio
L=sqrt(S*AR/2);                     %Length of rotor
R=S/(2*L);                          %Radius of rotor
w=TSR*V0/R;
coord = input('Enter NACA 4-digit Foil ', 's');%Hydrofoil like NACA 00XX
N= input('Enter number of blades ');
Sol =input('Enter Solidity Value ');
c = Sol*R/N;
Ao=input('Enter initial blade angle given ');
%-------------------------------------------------------------------------%
```

Upstream Calculations:

```
i=0;

while(i~=n)
i=i+1;
au=1.01;                            %Upstream interference factor
newau=1.0;
```

```
while (au-newau)>1e-3
au=newau;
Vu=au*V0;                          %Upstream velocity
Xt=R*w/Vu;                         %Local TSR
Wu=sqrt(Vu^2*((Xt-sin(thetau(i)))^2+(cos(thetau(i)))^2));%Relative velocity
Reb1=Wu*c/Kv;                      %Local Reynold number
Aoa=asin(((cos(thetau(i)))*cos(Ao*pi/180))/sqrt(((Xt-
sin(thetau(i)))^2+(cos(thetau(i)))^2))); % Angle of attack
[pol]=xfoil(coord,Aoa,Reb1,0,'oper iter 200');% Lift and drag co-efficient
function
Cnu=pol.CL*cosd(Aoa)+pol.CD*sind(Aoa);%Co-efficient of normal force upstream
Ctu=pol.CL*sind(Aoa)-pol.CD*cos(Aoa);%Co-efficient of tangential force upstream
g=@(thetau) (abs(sec(thetau)).*(Cnu.*cos(thetau)-
Ctu.*sin(thetau)).*(Wu./Vu).^2);   % Upwind function
y=quadl(g,-89*pi/180, 89*pi/180); %Upwind function integration
fup=N*c*y/(8*pi*R);                        %Upwind function value
newau=pi/(fup+pi);                                 %new upwind interference
factor
end
Auvector(i)=Aoa;
auvector(i)=newau;
Fnu (i) = (c*L/S)*Cnu*(Wu/V0)^2;%Normal Force
Ftu (i) = (c*L/S)*Ctu*(Wu/V0)^2;%Tangential Force
Tup (i) = 0.5*rho*c*R*L*Ctu*Wu^2;%Thrust Force
end
ts2 = trapz (thetau, Tup);%Summing all thrust forces
av_Tup = N*(ts2)/(2*pi);  %Average thrust force
av_Cqu = av_Tup/(0.5*rho*S*R*V0^2);
Cpu = av_Cqu*TSR;         %Power Co-efficient upstream
%-------------------------------------------------------------------------%
```

Downstream Calculations:

```
j=0;

while(j~=n)

j=j+1;

ad=1.01;
        %downstream interference factor

newad=1.0;

while (ad-newad)>1e-3

ad=newad;

Vd=ad*V0;
        %downstream velocity

Xt=R*w/Vd; %Local TSR

Wd=sqrt(Vd^2*((Xt-sin(thetad(j)))^2+(cos(thetad(j)))^2));%Relative velocity

Reb1=Wd*c/Kv; % Local Reynold number

Aoa=asin(((cos(thetad(j))*cos(Ao*pi/180)))/sqrt(((Xt-
sin(thetad(j)))^2+(cos(thetad(j)))^2)));%Angle of attack

[pol]=xfoil(coord,Aoa,Reb1,0,'oper iter 100');%Lift and drag co-efficient
function

Cnd=pol.CL*cosd(Aoa)+pol.CD*sind(Aoa);%Co-efficient of normal force

Ctd=pol.CL*sind(Aoa)-pol.CD*cos(Aoa);%Co-efficient of tangential force

g=@(thetad) (abs(sec(thetad)).*(Cnd.*cos(thetad)-
Ctd.*sin(thetad)).*(Wd./Vd).^2);%downwind function

y=quadl(g,91*pi/180, 269*pi/180); %downwind function integration

fwd=N*c*y/(8*pi*R); %downwind function value

newad=pi/(fwd+pi);  %new downwind interference factor

end

Advector(j)=Aoa;

advector(j)=newad;

Fnd (j) = (c*L/S)*Cnd*(Wd/V0)^2; %Normal Force

Ftd (j) = (c*L/S)*Ctd*(Wd/V0)^2; %Tangential Force

Tdw (j) = 0.5*rho*c*R*L*Ctd*Wd^2; %Thrust Force

end

pause(1);
```

```
ts4 = trapz (thetad, Tdw); %summing all thrust forces
av_Twd = N*(ts4)/(2*pi); %Average thrust force
av_Cqd = av_Twd/(0.5*rho*S*R*V0^2);
Cpd = av_Cqd*TSR; %Power Co-efficient downstream
```

End:

```
CP= Cpu+Cpd;  % Summing Upwind and downwind Power Co-efficient
```

Published with MATLAB® R2015a

APPENDIX II: MATLAB CODE FOR VLAUES OF C_L AND C_D

VALUES OF ANY HYDROFOIL

Written with courtesy of Copyright (c) 2015, Luca Virtuani from MatLAB

```
function [var] = xhydrofoil(coord,alpha,Re,Mach,varargin)


% Some default values
if ~exist('coord','var'), coord = 'NACA0012'; end;
if ~exist('alpha','var'), alpha =0;    end;
if ~exist('Re','var'),    Re =10000;      end;
if ~exist('Mach','var'),  Mach = 0;    end;
Nalpha = length(alpha); % Number of alphas swept
% default hydrofoil name
hydrofoil_name = mfilename;


% default filenames
wd = fileparts(which(mfilename)); % working directory, where xhydrofoil.exe
needs to be
fname = mfilename;
file_coord= [hydrofoil_name '.hydrofoil'];


% Save coordinates
if ischar(coord),  % Either a NACA string or a filename
  if isempty(regexpi(coord,'^NACA *[0-9]{4,5}$')) % Check if a NACA string
%     hydrofoil_name = coord; % some redundant code removed to go green (
~isempty if uncommented)
%   else             % Filename supplied
    % set coord file
    file_coord = coord;
  end;
```

```
else
  % Write hydrofoil ordinate file
  if exist(file_coord,'file'),  delete(file_coord); end;
  fid = fopen(file_coord,'w');
  if (fid<=0),
    error([mfilename ':io'],'Unable to create file %s',file_coord);
  else
    fprintf(fid,'%s\n',hydrofoil_name);
    fprintf(fid,'%9.5f   %9.5f\n',coord');
    fclose(fid);
  end;
end;

% Write xhydrofoil command file
fid = fopen([wd filesep fname '.inp'],'w');
if (fid<=0),
  error([mfilename ':io'],'Unable to create xhydrofoil.inp file');
else
  if ischar(coord),
    if ~isempty(regexpi(coord,'^NACA *[0-9]{4,5}$')),  % NACA string supplied
      fprintf(fid,'naca %s\n',coord(5:end));
    else  % filename supplied
      fprintf(fid,'load %s\n',file_coord);
    end;
  else % Coordinates supplied, use the default filename
    fprintf(fid,'load %s\n',file_coord);
  end;
  % Extra Xhydrofoil commands
  for ii = 1:length(varargin),
    txt = varargin{ii};
    txt = regexprep(txt,'[ \\\/]+','\n');
    fprintf(fid,'%s\n\n',txt);
  end;
```

```
  fprintf(fid,'\n\noper\n');
  % set Reynolds and Mach
  fprintf(fid,'re %g\n',Re);
  fprintf(fid,'mach %g\n',Mach);

  % Switch to viscous mode
  if (Re>0)
    fprintf(fid,'visc\n');
  end;

  % Varar accumulation
  fprintf(fid,'pacc\n\n\n');
  % Xhydrofoil alpha calculations
  [file_dump, file_cpwr] = deal(cell(1,Nalpha)); % Preallocate cell arrays

 for ii = 1:Nalpha
    % Individual output filenames
    file_dump{ii} = sprintf('%s_a%06.3f_dump.dat',fname,alpha(ii));
    file_cpwr{ii} = sprintf('%s_a%06.3f_cpwr.dat',fname,alpha(ii));
    % Commands
    fprintf(fid,'alfa %g\n',alpha(ii));
   fprintf(fid,'dump %s\n',file_dump{ii});
    fprintf(fid,'cpwr %s\n',file_cpwr{ii});
end
  % Varar output filename
  file_pwrt = sprintf('%s_pwrt.dat',fname);
  fprintf(fid,'pwrt\n%s\n',file_pwrt);
  fprintf(fid,'plis\n');
  fprintf(fid,'\nquit\n');
  fclose(fid);

  % execute xhydrofoil
  cmd = sprintf('cd %s && xhydrofoil.exe < xhydrofoil.inp > xhydrofoil.out
&',wd);
```

```
  [status,result] = system(cmd);
  if (status~=0),
     disp(result);
     error([mfilename ':system'],'Xhydrofoil execution failed! %s',cmd);
    return;
  else

  % Read dump file
  %    #    s        x        y     Ue/Vinf    Dstar     Theta      Cf       H
  jj = 0;
  ind = 1;
% Note that
hydrofoil.alpha = zeros(1,Nalpha); % Preallocate alphas
% Find the number of panels with an inital run
only = nargout; % Number of outputs checked. If only one left hand operator
then only do varar
%{
if only >1 % Only do the hydrofoil calculations if more than one left hand
operator is specificed
  for ii = 1:Nalpha
    jj = jj + 1;

    fid = fopen([wd filesep file_dump{ii}],'r');
    if (fid<=0),
      error([mfilename ':io'],'Unable to read xhydrofoil output file
%s',file_dump{ii});
    else
      D = textscan(fid,'%f%f%f%f%f%f%f%f','Delimiter','
','MultipleDelimsAsOne',true,'CollectOutput',1,'HeaderLines',1);
      fclose(fid);
      delete([wd filesep file_dump{ii}]);

      if ii == 1 % Use first run to determine number of panels (so that NACA
airhydrofoils work without vector input)
```

```
         Npanel = length(D{1}); % Number of airhydrofoil panels pulled from the
first angle tested

         % Preallocate Outputs

         [hydrofoil.s, hydrofoil.x, hydrofoil.y, hydrofoil.UeVinf,
hydrofoil.Dstar, hydrofoil.Theta, hydrofoil.Cf, hydrofoil.H] =
deal(zeros(Npanel,Nalpha));

      end


      % store data

      if ((jj>1) && (size(D{1},1)~=length(hydrofoil(ind).x)) &&
sum(abs(hydrofoil(ind).x(:,1)-size(D{1},1)))>1e-6 ),

        ind = ind + 1;

        jj = 1;

      end;

      hydrofoil.s(:,jj) = D{1}(:,1);

      hydrofoil.x(:,jj) = D{1}(:,2);

      hydrofoil.y(:,jj) = D{1}(:,3);

      hydrofoil.UeVinf(:,jj) = D{1}(:,4);

      hydrofoil.Dstar(:,jj) = D{1}(:,5);

      hydrofoil.Theta(:,jj) = D{1}(:,6);

      hydrofoil.Cf(:,jj) = D{1}(:,7);

      hydrofoil.H (:,jj)= D{1}(:,8);

    end;


    hydrofoil.alpha(1,jj) = alpha(jj);


    % Read cp file

    fid = fopen([wd filesep file_cpwr{ii}],'r');

    if (fid<=0),

      error([mfilename ':io'],'Unable to read xhydrofoil output file
%s',file_cpwr{ii});

    else

      C = textscan(fid, '%10f%9f%f', 'Delimiter', '', 'WhiteSpace', '',
'HeaderLines' ,3, 'ReturnOnError', false);

      fclose(fid);
```

```
      delete([wd filesep file_cpwr{ii}]);
      % store data
      if ii == 1 % Use first run to determine number of panels (so that NACA
airhydrofoils work without vector input)
         NCp = length(C{1}); % Number of points Cp is listed for pulled from
the first angle tested
         % Preallocate Outputs
         [hydrofoil.xcp, hydrofoil.cp] = deal(zeros(NCp,Nalpha));
         hydrofoil.xcp = C{1}(:,1);
      end
      hydrofoil.cp(:,jj) = C{3}(:,1);
    end;
  end;
end
%}
if only <= 1% clear files for default run
for ii=1:Nalpha
delete([wd filesep file_dump{ii}]);
delete([wd filesep file_cpwr{ii}]);
end
end
  fid = fopen([wd filesep file_pwrt],'r');
  if (fid<=0),
       var.alpha =0;
    var.CL  = 0;
    var.CD  = 0;
    var.CDp = 0;
    var.Cm  = 0;
    var.Top_xtr = 0;
    var.Bot_Xtr = 0;
  system('close.bat');
  system('cmdexe.bat');
  else
```

```
    P = textscan(fid,' Calculated varar for: %[^\n]','Delimiter',' 
','MultipleDelimsAsOne',true,'HeaderLines',3);
    var.name = strtrim(P{1}{1});


    P = textscan(fid, '%*s%*s%f%*s%f%s%s%s%s%s%s%s', 1, 'Delimiter', ' ', 
'MultipleDelimsAsOne', true, 'HeaderLines', 2, 'ReturnOnError', false);
    var.xtrf_top = P{1}(1);
    var.xtrf_bot = P{2}(1);
    P = textscan(fid, '%*s%*s%f%*s%*s%f%*s%f%*s%*s%f', 1, 'Delimiter', ' ', 
'MultipleDelimsAsOne', true, 'HeaderLines', 0, 'ReturnOnError', false);
    var.Re = P{2}(1) * 10^P{3}(1);
    var.Ncrit = P{4}(1);
    P = textscan(fid, '%f%f%f%f%f%f%f%*s%*s%*s%*s', 'Delimiter',  ' ', 
'MultipleDelimsAsOne', true, 'HeaderLines' , 4, 'ReturnOnError', false);
    fclose(fid);
    delete([wd filesep file_pwrt]);
    var.alpha = P{1}(:,1);
    var.CL  = P{2}(:,1);
    var.CD  = P{3}(:,1);
    var.CDp = P{4}(:,1);
    var.Cm  = P{5}(:,1);
    var.Top_xtr = P{6}(:,1);
    var.Bot_Xtr = P{7}(:,1);
     system('close.bat');
  system('cmdexe.bat');
  end
 if length(var.alpha) ~= Nalpha % Check if xhydrofoil failed to converge
%{
Cl=0;Cd=0;
 fid1 = fopen([wd filesep fname '.out'],'r');% This opens a file
n = 0;
tline = fgetl(fid1);
while ischar(tline)
  tline = fgetl(fid1);
  n = n+1;
```

```
end
l=29; %no of lines from end
 i=0;
 j=n-l;
    i=0;
    fid1 = fopen([wd filesep fname '.out'],'r'); % This opens a file


    while i<j
        l1=fgetl(fid1); % anytime you use fgetl you read a line and next time
you use it reads next
    i=i+1;
    end
         disp(['L1=',l1]);
C = textscan(l1,'%s %f32 %s %f32','Delimiter','=');
l2=fgetl(fid1);
disp(['L2=',l2]);
D = textscan(l2,'%s %s %f32 %s %s %f32');
fclose(fid1);
a = C{3};
var.CL = C{4};
Cm = D{3};
%checking CD value
if isempty(D{6})
    var.CD=0;
else
var.CD = D{6};
end
 %}
  warning('One or more alpha values failed to converge. Last converged was
alpha = %f. Rerun with ''oper iter ##'' command.\n')
    var.alpha =0;
    var.CL  = 0;
    var.CD  = 0;
    var.CDp = 0;
```

```
    var.Cm  = 0;
    var.Top_xtr = 0;
    var.Bot_Xtr = 0;
     system('close.bat');
  system('cmdexe.bat');
 end
  end
  pause(1);
end
```

Published with MATLAB® R2015a